ICC-IMR FY2025

Activity Report

International Collaboration Center

Institute for Materials Research
Tohoku University

ICC-IMR

https://www.icc-imr.imr.tohoku.ac.jp/

CONTENTS

Mission

The ICC-IMR was founded in April 2008 as the center for international collaboration of the Institute for Materials Research (IMR) a center of excellence in material science, consisting of 27 research groups and six research centers. The ICC-IMR works as a gateway of diverse collaborations between overseas and IMR researchers. The ICC-IMR has invited 101 visiting professors and conducted 26 international research projects since its start-up (please inspect the graph below for more details,). The applications are open to foreign researchers and the projects are evaluated by a peer-review process involving international reviewers.

ICC-IMR coordinates five different programs:

1) International Integrated Project Research
2) Visiting Professorships
3) International Workshops
4) Fellowships for Young Researcher and PhD Student
5) Material Transfer Program

We welcome applicants from around the globe to submit proposals!

Visitors supported by ICC-Programs

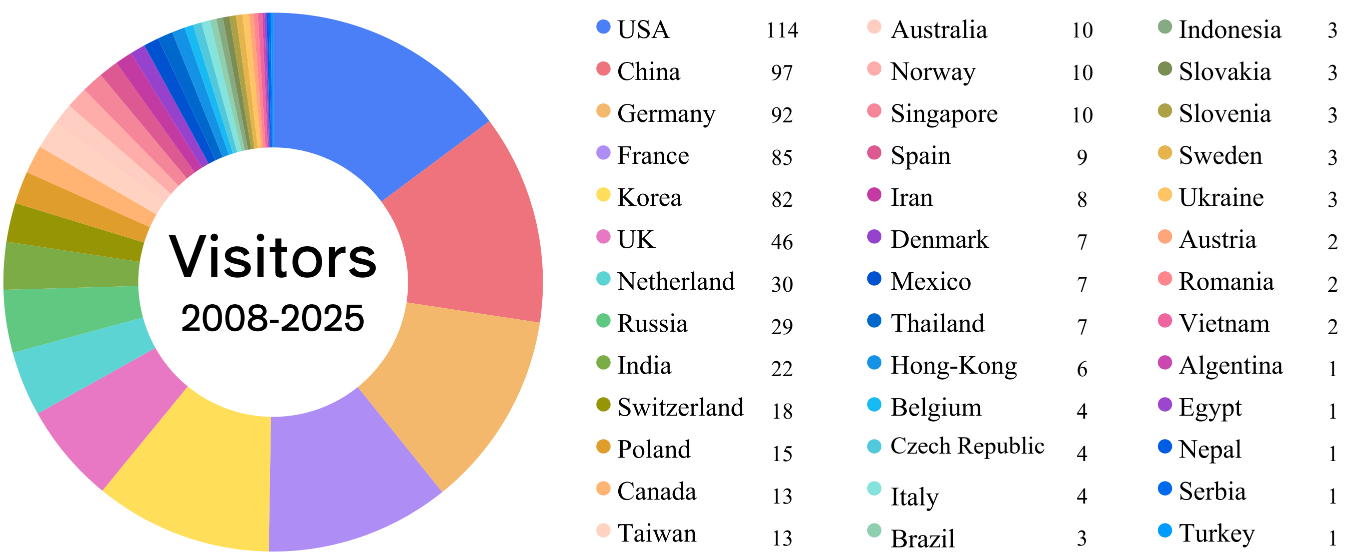

ICC-IMR COMMITTEE MEMBERS

Director

Prof. Hiroyuki NOJIRI

Steering Committee

Prof. Kozo FUJIWARA

Prof. Eiji AKIYAMA

Prof. Dai AOKI

Prof. Hidemi KATO

Prof. Yusuke NOMURA

Prof. Yoshinori ONOSE

Prof. Masashi WATANABE

Visiting Professors

Accepted No.	Title in IMR・Name・Affiliation	Proposed Research	Host	Term
24G3	Visit. Assis. Prof. Dr. Yida Xiong・Nanyang Technological University, Singapore/Sun Yat-sen University, China	Corrosion/Stress Corrosion Cracking Behaviors of Binder Jet Printed and Conventionally Manufactured 316L Stainless Steel	Prof. Akiyama	2024.7.1-2025.6.30
24G7	Visit. Assis. Prof. Dr. Qun Niu・Hefei Institutes of Physical Science, Chinese Academy of Sciences, China	Thermoelectric Study of Two-Dimensional Heavy Fermions	Prof. Aoki	2025.1.1-2025.12.31
24G8	Visit. Assoc. Prof. Dr. Oleg Tretiakov・UNSW Sydney, Australia	Synthetic Antiferromagnet Spintronics	Prof. Nojiri	2025.3.3-2025.5.9
25G1	Visit. Prof. Dr. Marcel Somers・Technical University of Denmark	Reconciling Martensite Formation in the Sub-Zero Celsius Regime with the Theory of Martensite Formation in Steels. Gaseous Nitriding of Iron-Based Alloys; Microstructure Evolution and Residual Stress.	Prof. Furuhara	2025.8.25-2025.9.26
25G2	Visit. Prof. Dr. Ilya Sheikin ・LNCMI, CNRS, France	Single Crystal Growth and Electronic Properties of Layered U- and Ce-Based Compounds	Prof. Aoki	2025.6.1-2025.8.29
25G3	Visit. Prof. Dr. Eun-Ae Choi・Korea Institute of Materials Science, Korea	Design of High-Strength, High-Conductivity Copper Alloys Through Controlling the Precipitation Behavior Based on First-Principles Calculations	Prof. Kato	2025.7.11-2025.9.10
25G4	Visit. Assoc. Prof. Dr. Arnaud Joel Badel・CNRS, France	High Temperature Superconducting Magnet Developments for 40T-CSM	Prof. Awaji	2025.7.1-2026.6.30
25G5	Visit. Prof. Dr. Del Atkinson・Durham University, UK	Spintronic Multilayers for Energy Efficient Electronic Memory Applications	Prof. Seki	2025.11.4-2026.1.30
25G6	Visit. Prof. Dr. William Knafo・LNCMI- Toulouse, CNRS, France	Magnetization of UTe_2 in High Magnetic Fields	Prof. Aoki	2025.10.8-2025.11.27

Corrosion and Stress Corrosion Cracking Behaviors of Binder Jet Printed 316L

Introductory part,Abstract: This study systematically investigated the corrosion and stress corrosion cracking (SCC) behavior of binder jet-printed (BJP) 316L. The results confirmed that both inherent porosity and the presence of δ-ferrite have a detrimental impact on the material's resistance to both localized corrosion and SCC. To address this, hot isostatic pressing (HIP) and femtosecond laser texturing (FLT) were identified as effective methods for significantly improving these properties.

Binder jet printing technology is a type of additive manufacturing technology. Compared to traditional manufacturing methods, it offers unparalleled advantages in the design and manufacturing of complex components. In contrast to additive manufacturing techniques that use laser heat sources, metal materials produced by this technology contain almost no non-equilibrium microstructures [1].

It was confirmed that the binder-jet-printed 316L exhibited high porosity and δ-ferrite content. During immersion corrosion tests (25 wt% $MgCl_2$, 75 °C, 70% RH), these features induced localized corrosion (Fig. 1). Similarly, in the SCC tests under identical conditions, they initiated cracks and promoted crack propagation (Fig. 2).

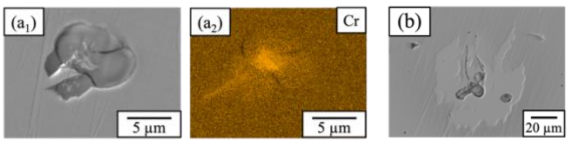

Fig. 1. Features of localized corrosion in the BJP specimens after immersion testing: (a_1, a_2) around the δ-ferrite, (b) around pores.

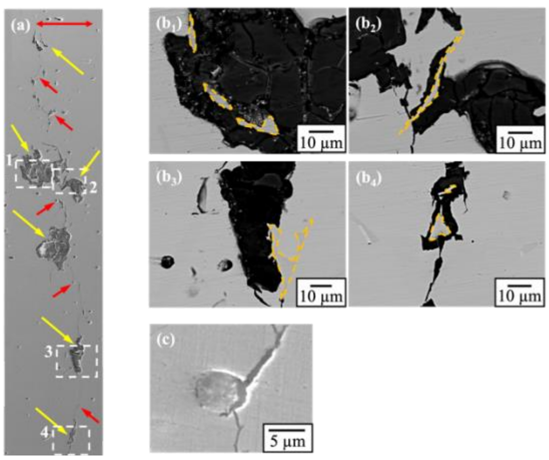

Fig. 2. (a) a crack observed in BJP specimens after SCC test. The yellow arrows in (a) indicate the pits formed around δ-ferrite, and the red arrows in (a) indicate the pores observed in the crack path. The yellow dotted curves in (b1-b4) indicate the δ-ferrite.

To address this, we implemented a HIP process (1160 °C, 104 MPa, 240 minutes), which effectively reduced porosity and the δ-ferrite content in the BJP 316L. This optimization led to a significant improvement in performance, as evidenced by the absence of any localized corrosion or stress corrosion cracking in subsequent tests.

We also applied Femtosecond Laser Texturing (FLT) to the surface of the BJP 316L (Fig. 3). This treatment induced superhydrophobicity, placing the material in a Cassie-Baxter state. This state retards the contact between the corrosive medium and the underlying bulk material, thereby improving the SCC resistance.

This research project led to two publications:

(1) ***Corrosion Science***, 2025, 252: 112968;

(2) ***Acta Materialia***, 2026, 302: 121615.

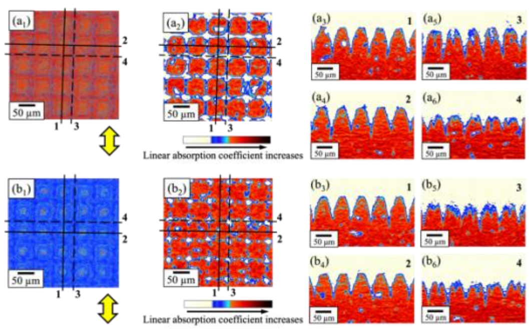

Fig. 3. Surface morphology of FLT-treated BJP 316L.

References

[1] T.H. Becker, P. Kumar, and U. Ramamurty, Fracture and fatigue in additively manufactured metals, Acta Mater. 219, 117240 (2021)

Keywords: Corrosion, Steel, Texture
Yida Xiong (Sun Yat-sen University)
E-mail: xiongyd6@mail.sysu.edu.cn

Thermoelectric Study of Two-dimensional Heavy Fermions

We measured the thermoelectric responses of the Cr-based Kagome material $CsCr_6Sb_6$ using a novel thermoelectric technique for nm-sized flakes. The temperature-dependent Seebeck and Nernst coefficients resemble those of the heavy fermion $CeCu_2Si_2$, indicating Kondo interactions near the 2D limit. Furthermore, by integrating this technique with diamond anvil cells, we resolved sub-nV signals in $CeSb_2$ up to 29 T under pressure. This establishes a robust probe for future studies and tuning of 2D heavy-fermion systems.

The recent realization of two-dimensional (2D) van der Waals heavy fermions provides a fertile ground for exploring enhanced quantum fluctuations and novel correlated phases, such as quantum criticality and unconventional superconductivity [1-5]. Yet, the advancement of this field is severely hindered because standard bulk experimental probes for heavy fermions are challenging to apply at the 2D limit. Here we developed the thermoelectric technique for nm-sized thin flakes which show potential for the studies and tuning of 2D heavy-fermions systems.

Fig.1 shows the Seebck (S) and Nernst (N) coefficient of a Kagome material $CsCr_6Sb_6$ thin flake as a function of temperature. Below T_F~70K, the onset of frustrated magnetism from the resistivity measurements [3], the S/T drops sharply to a minimum near the Kondo temperature T_N~28 K, then rapidly increases and change sign below 10 K. Concurrently, the 12 T Nernst signal peaks sharply near T_N, with the maximum value reaching 1 $\mu V/K$. These temperature profile of S/T and N closely resemble those of the famous heavy fermion $CeCu_2Si_2$, providing compelling evidence for Kondo interactions approaching the 2D limit.

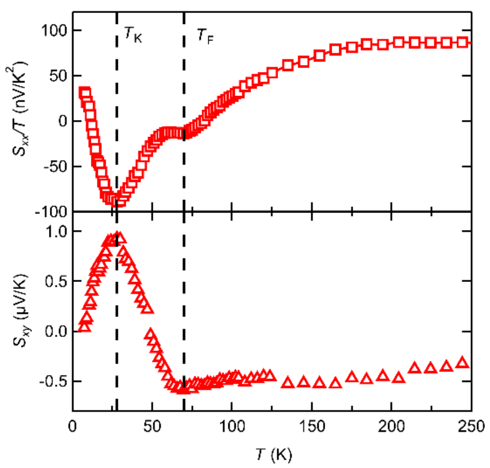

Fig. 1 The temperature dependent Seebeck and Nernst coefficient of $CsCr_6Sb_6$ thin flakes. The Seebeck was measured at 0 T while the Nernst effect was measured at 12 T.

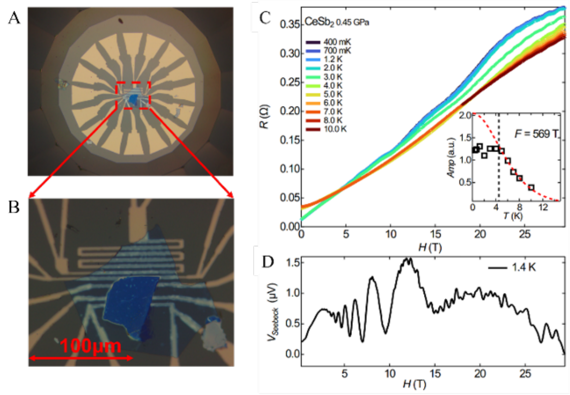

Fig. 2(A-B) The pre-patterned electrodes for thermoelectric measurements on the top of a diamond anvil. (C-D) The resistance and Seebeck coefficient of $CeSb_2$ under pressure.

Fig. 2A and 2B details the integration of the same methodology in a diamond anvil cell, enabling simultaneous resistivity and thermoelectric power measurements of a thin flake under pressure. Tested under high magnetic field up to 29 T in a ^{3}He calorimeter, the Seebeck coefficient of the heavy fermion compound $CeSb_2$ achieves sub-nanovolt precision (Fig. 2D). It reveals pronounced quantum oscillations starting from 2 T, which match the frequencies from resistivity but offer significantly better resolution. This establishes the superior capability of our thermoelectric technique for probing 2D heavy fermions under pressure.

This work was performed in collaboration with D. Aoki, and A. Miyake (Tohoku University), and T. F. Poon, and S. K. Goh (The Chinese University of Hong Kong), and A. Pourret, and G. Knebel (CEA Grenoble), and G. Seyfarth (LNCMI Grenoble).

References

[1] V. A. Posey *et al.*, Nature **625**, 483 (2024).
[2] A. Fumega & J. Lado, Nano Lett. 2024, 4272-4278 (2024)
[3] B. Song *et al.*, Nat. Commun. **16**, 5643 (2025)
[4] H. Lee et al. arXiv:2509.04902 (2025)
[5] T. Shi et al. arXiv: 2601.18476 (2026)
[6] P. Sun & F. Steglich, Phys. Rev. Lett. 110, 216408 (2013)

Keywords: van der Waals heavy fermion; Thermoelectricity; nano device;
Qun Niu (High Magnetic Field Laboratory, HFIPS, CAS)
E-mail: qniu@hmfl.ac.cn
http://

Synthetic Antiferromagnet Spintronics

Abstract: We investigate the dynamics of bimerons and skyrmions in synthetic antiferromagnets. Synthetic antiferromagnets are advantageous for decreasing the bimeron and skyrmion Hall angles and enabling texture detection through local magnetization, bypassing the need to rely on the Neel order parameter. Using micromagnetic simulations and Thiele's equation approach we calculated the bimeron/skyrmion Hall angles.

Motivated by the differences between of skyrmions and their in-plane magnetized analogues – bimerons – in synthetic antiferromagnets (SAFs), we investigated their current-driven dynamics employing micromagnetic simulations and analytical Thiele's equation approach. We considered SAF structures consisting of several antiferromagnetically coupled layers. For bimerons, we considered additional ferromagnetic layers with fixed in-plane magnetization adjoined to the SAF, see Fig. 1.

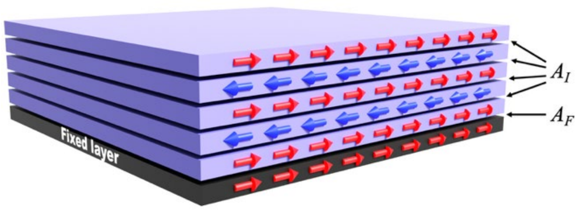

Fig. 1 Schematic representation of a 5-layer SAF for bimerons stabilization with one fixed layer.

In this case, the effect of exchange bias from the fixed layer is similar to a magnetic field, i.e., increasing the strength of exchange bias reduces the bimeron's size in the adjacent layer. This translates through the rest of SAF via interlayer antiferromagnetic exchange. Since the strength of the exchange bias can be modified by changing interlayer exchange coupling between a fixed layer and the SAF, this configuration offers additional control over the size of the spin texture and its motion. However, since this effect diminishes with distance from the fixed layer, bimerons are smaller at the bottom and become larger at the top layers of the SAF. To prevent this asymmetry and increase the number of layers where the bimeron size is controlled by this effect, we also considered a configuration with the second fixed layer added on top of the SAF.

We have shown that in the uncompensated SAFs, bimeron and skyrmion Hall effects diminish in the bulk limit, which can be understood by the decrease in the averaged topological charge with increasing the number of layers. However, bimeron/skyrmion Hall angles have a quite nonmonotonic dependence on number of layers N with an extremum for a certain N. The bimeron (skyrmion) Hall effect vanishes for compensated SAFs with two fixed layers, whereas the SAFs with only one fixed layer exhibit nonzero Hall angles, which becomes more evident when interlayer exchange interaction is weak. Remarkably, we identified the conditions when bimerons and skyrmions in uncompensated SAFs can move faster than in antiferromagnets. Depending on spin-transfer torque strength, spin texture velocities in uncompensated SAFs increase or decrease with the number of layers. Finally, we have studied finite temperature effects on bimeron and skyrmion dynamics and stability in SAFs by employing stochastic Landau-Lifshitz-Gilbert equation with white-noise correlated random magnetic fields. Our findings offer a comprehensive understanding of the topological magnetic texture dynamics in SAFs, which is essential for designing topological spin-texture based logic and memory nanodevices.

Furthermore, the interplay of these spin textures with spin-orbit coupled substrates [1] would be interesting to study as well in SAFs, since the previous studies mainly focused on the Hall responses of skyrmions coupled to heavy-metal substrates. Finally, this study can be extended to the investigation of domain-wall bimerons [2] and their dynamics in synthetic antiferromagnets. These findings will deepen the understanding of SAF dynamics and offer guidance for their implementation in skyrmion- and bimeron-based spintronic devices.

References

[1] Z. Llewellyn, E. Mascot, O. A. Tretiakov, and S. Rachel, Phys. Rev. B 112, 155417 (2025).

[2] J. Chen, L. Shen, Y. Zhou, O. A. Tretiakov, and X. Li, arXiv:2505.00959; Phys. Rev. B, accepted (2025).

Keywords: spintronics, magnetic properties, spin transfer
Oleg A. Tretiakov (University of New South Wales, Sydney, Australia)
E-mail: o.tretiakov@unsw.edu.au
https://sites.google.com/site/tretiakov/

Reconciling martensite formation in the sub-zero Celsius regime with the theory of martensite formation in steel

Abstract: The activities involved a thorough re-interpretation of an existing data set acquired on sub-zero Celsius martensitic transformation in a precipitation-hardening stainless steel with different nitrogen contents. The martensitic transformation was monitored with magnetometry as austenite is paramagnetic and martensite is ferromagnetic.

The temperature below which martensite forms from austenite during continuous cooling was tailored by deliberate addition of nitrogen to 17-4 PH steel. More nitrogen leads to a lower threshold temperature below martensite forms, referred to as martensite start M_s. Martensitic transformation can occur athermally, i.e. during cooling, or isothermally. The morphology of the forming martensite depends on the nitrogen content and the cooling rate (among others). For relatively low nitrogen contents, the morphology of martensite is referred to as lath martensite. This martensite has an internal structure of dislocations necessary to accommodate the transformation strain occurring on transforming the parent fcc crystal lattice into the bcc martensite lattice. For higher nitrogen contents also plate martensite forms, which is internally twinned. This latter transformation is observed to be accompanied by bursts in the transformation rate as measured with in-situ magnetometry measurements (Fig. 1). Isothermal transformation at temperatures above M_s shows mainly lath martensite which appears thermally activated. For a nitrogen content of 0.20 wt%, plate martensite can form isothermally at a very low temperature. For intermediate nitrogen contents, plate martensite can be preceded by lath martensite, while on heating from boiling nitrogen temperature previously formed martensite plates appear to act as nucleation sites for thermally activated martensite with an internally dislocated structure, thereby developing into lenticular martensite. The observations were rationalized by relating M_s to the driving force for martensite formation. In the temperature range (i.e. coupled nitrogen content and M_s) where lath martensite forms athermally, M_s depends strongly on nitrogen content; for the regime where plate martensite forms athermally this dependence is less pronounced (Fig. 2). This observation correlates with the temperature dependence of the critical resolved shear stress for dislocation generation/movement (the internal structure in laths) and for twinning (the internal structure in plate martensite) in the bcc crystal structure. The first is strongly temperature dependent, the second is not. This interpretation is also consistent with thermally activated (isothermal) martensite being generally of lath type and thermally activated martensite forming during heating. The origin of thermal activation is most likely the movement of screw dislocations in the bcc lattice.

Additionally, unique results obtained at European Synchrotron Radiation Facility (ESRF) with Dark Field X-ray Microscopy on in-situ isothermal martensite formation were reinterpreted. The data set provides information on lattice rotation, as a measure for plastic strain, and the distribution of elastic residual stress in the remaining austenite.

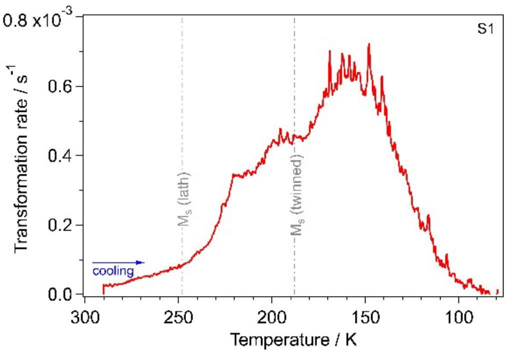

Fig. 1 Transformation rate obtained from in-situ magnetometry measurements in dependence of temperature during isochronal cooling for a specimen with 0.08 wt% N (S1). For temperatures below 189 K (M_s for twinned martensite) bursts appear.

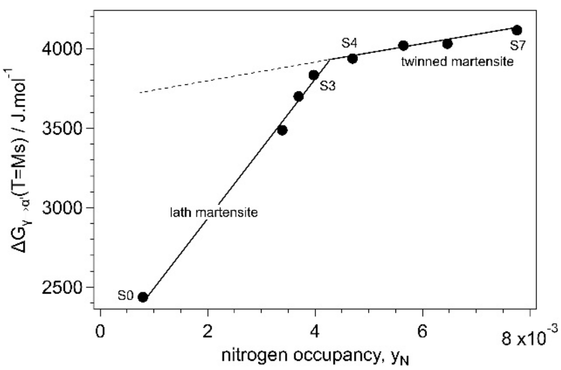

Fig.2 Dependence of the driving force for martensite formation at M_s in dependence of the nitrogen occupancy of octahedral interstices in austenite. During cooling the driving force increases. For samples S0-S3 first lath martensite forms, thereafter plate (twinned); for S4-S7 plate martensite forms immediately.

Keywords:phase transformation, steel, kinetics
Marcel A.J. Somers, Technical University of Denmark
E-mail: majs@dtu.dk
http://construct.dtu.dk

Unusual magnetic phase diagram and magnetic structure of the field-induced phases in Ce_2RhIn_8

Our recent high-field specific-heat measurements on a single crystal of Ce_2RhIn_8 grown in Oarai revealed unusual magnetic phase diagrams, including field-induced phases for magnetic fields applied along both principal crystallographic directions (the c and *a* axes). Motivated by these observations, we carried out low-field specific-heat and magnetization measurements with the field applied along the [110] direction. Unexpectedly, the resulting phase diagram differs significantly from that observed for fields along [100]. Moreover, our first neutron-diffraction experiment with the field applied along [110] uncovers a magnetic structure more complex than previously established, even in zero field. We further track the evolution of this structure across the field-induced phases.

The antiferromagnetic heavy-fermion compound Ce_2RhIn_8 belongs to the same family as, and shares several similarities with, the well-studied prototypical material $CeRhIn_5$, which exhibits a unique behavior under applied magnetic field [1]. Ce_2RhIn_8 crystallizes in a tetragonal structure and undergoes an antiferromagnetic (AFM) transition at a Néel temperature of T_N = 2.8 K [2]. Single-crystal neutron diffraction has established a commensurate magnetic structure with propagation vector **Q** = (1/2, 1/2, 0) and a staggered magnetic moment of 0.55μ_B [3].

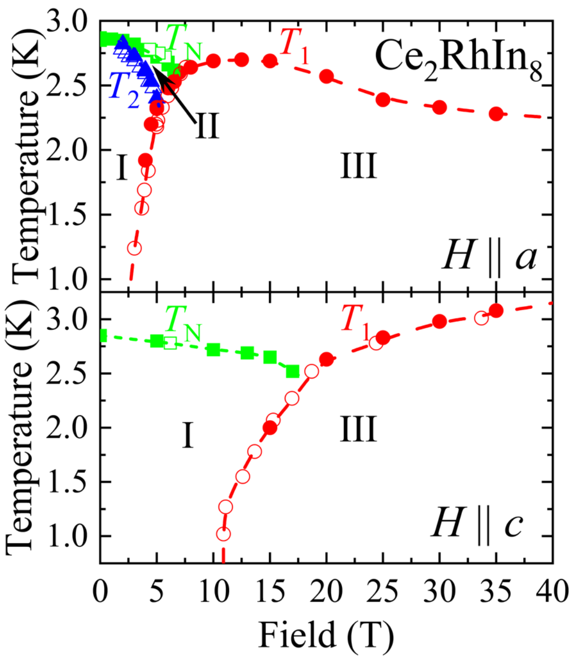

Fig. 1 Magnetic phase diagram of Ce_2RhIn_8 obtained from specific-heat measurements performed as a function of temperature (solid symbols) and magnetic field (open symbols) for the field applied along the *a* (upper panel) and c (lower panel) axis. Lines are a guide for the eye.

Recently, we performed specific-heat measurements on a high-quality single crystal of Ce_2RhIn_8 grown in Oarai, in magnetic fields up to 35 T applied along both principal crystallographic directions. The resulting phase diagrams are shown in Fig. 1. When the magnetic field is applied along the *a* axis, two additional field-induced AFM phases are observed, in agreement with previous reports. One of these phases is confined to a small region of the field–temperature phase diagram. The other, which develops above ≈2.5 T, is remarkably robust: its transition temperature increases with increasing field, reaches a maximum at ≈12 T, and subsequently decreases, although it tends to saturate toward the highest fields of our measurements.

For a field applied along the c axis, T_N initially decreases with field, as expected for a typical antiferromagnet. Surprisingly, an additional phase emerges above ≈10 T, which is likely of the same origin as the phase observed above 2.5 T for the other field orientation. This phase is also unusually robust: its transition temperature continues to increase up to 35 T, where it exceeds the zero-field T_N. These results were published in Ref. [4].

To understand the origin of the field-induced phases, it is essential to determine their magnetic structure by neutron diffraction. However, such measurements under magnetic field are only feasible when the field is applied along the [110] direction. For this reason, we performed low-field specific-heat and magnetization measurements with the field applied along this direction. Surprisingly, the resulting phase diagram (Fig. 2) differs strongly from that for the field applied along the [100] direction (the *a* axis). For comparison, in $CeRhIn_5$, the phase diagrams are identical for fields applied along the [100] and [110] directions.

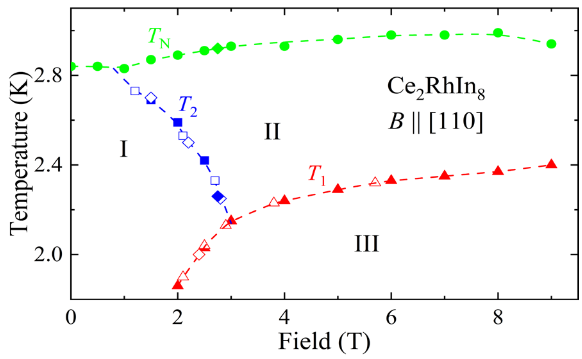

Fig. 2 Magnetic phase diagram of Ce_2RhIn_8 obtained from specific-heat (circles, squares, and triangles) and magnetization (diamonds) measurements performed as a function of temperature (solid symbols) and magnetic field (open symbols) for the field applied along the [110] direction. Lines are a guide for the eye.

Once the low-field magnetic phase diagram for the field along [110] was established, we performed in-field neutron diffraction experiments at JAEA–Tokai. Quite surprisingly, even in zero magnetic field (phase I), we observed an incommensurate wave vector **Q** = (0.46, 0.46, 0) in addition to the previously reported commensurate vector **Q** = (0.5, 0.5, 0). However, at zero field, the commensurate phase is dominant. The situation reverses in phase III, where the intensity of the incommensurate Bragg peak exceeds that of its commensurate counterpart. Finally, in phase II, the commensurate phase is suppressed, leaving only the incommensurate phase.

We also attempted to extend the phase diagram to higher fields using pulsed-field magnetization measurements at the ISSP, University of Tokyo. Unfortunately, this experiment was unsuccessful, as no anomalies were detected at high fields. However, specific-heat measurements in fields up to 36 T are planned at LNCMI–Grenoble to extend the phase diagram for the field along [110] to higher fields. Finally, we plan to perform NMR measurements at JAEA–Tokai to provide further insight into the field-induced phases, particularly for fields applied along the [100] and [001] directions, which are inaccessible to neutron diffraction.

This work was performed in collaboration with D. Aoki, A. Miyake, and A. Nakamura (Tohoku University), and K. Kaneko, Y. Hirose, and C. Tabata (JAEA-Tokai).

References

[1] S. Mishra *et. al.*, Phys. Rev. B **103**, 045110 (2021).
[2] J. Thompson *et. al.*, J. Magn. Magn. Mater. **226-230**, 5 (2001).
[3] W. Bao *et. al.*, Phys. Rev. B **64**, 020401 (2001).
[4] T. Klein *et. al.*, Phys. Rev. B **111**, L201110 (2025).

Keywords: heavy fermion, magnetic properties, neutron diffraction
Ilya Sheikin (LNCMI-Grenoble, CNRS)
E-mail: ilya.sheikin@lncmi.cnrs.fr
http://

Design of High-Strength, High-Conductivity Copper Alloys through Controlling the Precipitation Behavior based on First-Principles Calculations

We investigated precipitation control in Cu-Ti alloys using first-principles calculations to design high-strength, high-conductivity copper alloys. DFT analysis of 22 elements revealed that P and Cr can enhance the cohesive energy of α-Cu_4Ti, reduce its precipitation activation energy, and refine its precipitate size, thereby promoting α-Cu_4Ti precipitation. These insights provide guidance for tailoring precipitation behavior in the development of advanced Cu-Ti alloys.

Cu-Ti alloys can reach tensile strengths above 1 GPa, which makes them promising alternatives to Cu–Be alloys [1]. Aging causes spinodal decomposition, forming metastable α-Cu_4Ti (I4/m) as the strengthening phase, later transforming into β-Cu_4Ti (Pmmn) [2,3]. Due to slow precipitation, optimizing strength and conductivity is difficult. Precipitation behavior depends on cohesive and interfacial energies of α-Cu_4Ti with the Cu matrix. Previous DFT work on 3d transition metals [4] examined these separately but not their combined effect.

Here, we calculate these energies for α-Cu_4Ti doped with 22 alloying elements (Li, Mg, Al, Si, P, Sc, V, Cr, Mn, Fe, Co, Ni, Zn, Ga, Ge, Y, Zr, Nb, Mo, In, Sn, Hf), derive precipitation activation energy and critical length, and identify elements that promote finer precipitation. First-principles DFT with PAW and PBE in VASP was used. Supercells for bulk α-Cu_4Ti and two major interfaces with Cu were fully relaxed. Alloying elements were substituted into Cu or Ti sites at 6.25 at.%.

Twelve elements (P, Cr, Mn, Fe, Co, Ni, Mo, Li, Sc, Y, Zr, and Hf) increased cohesive energy (E_{coh}), stabilizing α-Cu_4Ti. Mn was effective at both sites. Interfacial energies (E_{int}) were computed for Cu (001) // α-Cu_4Ti (001) and Cu (310) // α-Cu_4Ti (100). Among twelve dopants enhancing E_{coh}, only P and Cr lowered E_{int} at Cu (001) // α-Cu_4Ti (001) interface by relieving lattice mismatch, but increased it at Cu (310) // α-Cu_4Ti (100).

Total energy curves combining E_{coh} and E_{int} were analyzed against precipitate size. Figure 1, for Cr-doped α-Cu_4Ti, shows reduced precipitation activation energy (E_a) and critical length (L_c) compared with undoped alloy. P and Cr lowered E_a by 21% and 37% and reduced L_c by 11% and 26%, forming smaller, more uniform precipitates. Mn, Co, and Ni increased E_a but reduced L_c, indicating some refinement effect.

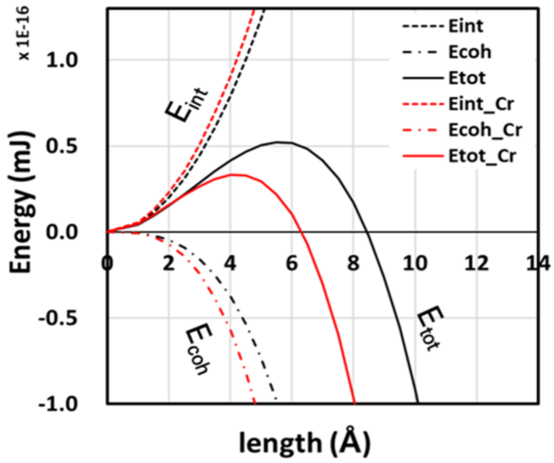

Fig. 1 The cohesive, interfacial and total energies for α-$(Cu_{0.94}Cr_{0.06})_4Ti$ as a function of the length of precipitate. The black line represents the energies of the undoped one.

In conclusion, P and Cr are the most effective additives, stabilizing α-Cu_4Ti and enhancing precipitation, offering a pathway to high-performance Cu-Ti alloys with tailored microstructures.

References

[1] S. Semboshi, Y. Kaneno, T. Takasugi, S. Z. Han and N. Masahashi, Metall. Mater. Trans. A, 50A, 1389-1396 (2019).
[2] W. A. Soffa and D. E. Laughlin, Progress in Materials Science, 49, 347-366 (2004)
[3] S. Semboshi, S. Sato, M. Ishikuro, K. Wagatsuma, A. Iwase and T. Takasugi, Metall. Mater. Trans. A, 45A, 3401-3411 (2014)
[4] E.-A. Choi, S. Z. Han, J. H. Ahn, S. Semboshi, Y. Kadoi, K. Kim and J. Lee, J. Jpn. Inst. Copper, 58, 23-27 (2019)

Keywords: ab inito calculation, alloy, second phases
Eun-Ae Choi (Korea Institute of Materials Science)
E-mail: eunae.choi@kims.re.kr

Study of voltage dynamics in large REBCO coils: Toward the protection of 33T then 40 T REBCO inserts

REBCO Coated Conductors inserts are mandatory for very high field superconducting magnets. Yet, the number of full-size HTS inserts implemented worldwide is limited so their long-term reliability is still largely unproven. In order to acquire enough feedback to safely operate the 33 T CSM at HFLSM and its future 40 T upgraded insert, extensive tests were conducted on the existing 20 stacked-pancake coil prototype. Its mechanical behavior at low temperature under high stress was already reported. In this work the transient voltages were studied during operation at variable temperatures up to its maximum operating current. This new understanding offers additional options for the design of future REBCO insert protection systems.

The robust REBCO insert coil concept [1] chosen for the design of the future 33 T then 40 T inserts at HFLSM features fully isolated turns to limit the transient losses and to achieve fast dynamics. Protection against thermal runaway relies on early detection of dissipative behaviour thanks to sensitive voltage detection, triggering discharge in dump resistor [2].

In order for such early detection scheme to be effective, a good understanding of the transient voltage dynamics. Voltage dynamics were extensively studied in [3] with help of transient modelling. It was observed that the total coil voltage can be separated basically in three components: inductive voltage, related to the field produced by the imposed circulating current in the coil, dissipating voltage due to dynamic current redistribution in the conductor cross-section, related to the shielding and coupling current induced field, and dissipation due to local overstepping of the critical current. Only the latter is a concern for coil safety and must be discriminated from the rest.

Pick up coils having a good coupling with the REBCO coils can be used to cancel out most of the inductive voltage. The obtained "compensated coil signal" is smaller and has reduced noise while still containing the signal of interest, that is, the coil dissipative voltage due to overstepping of the critical current. However, it still retains significant transient components due to dynamic current redistribution in the conductor cross section, which is hysteretic and makes it difficult to set

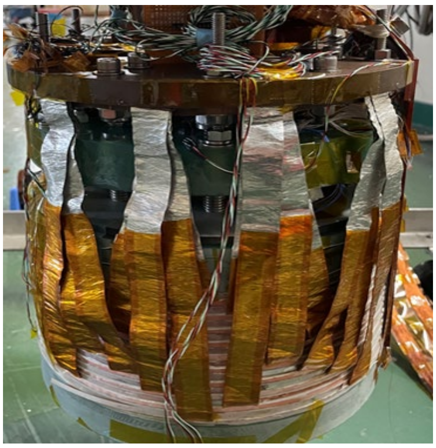

Fig. 1: 20-stacked pancake coil mounted on the cold plate of the HFLSM large bore conduction-cooled cryostat

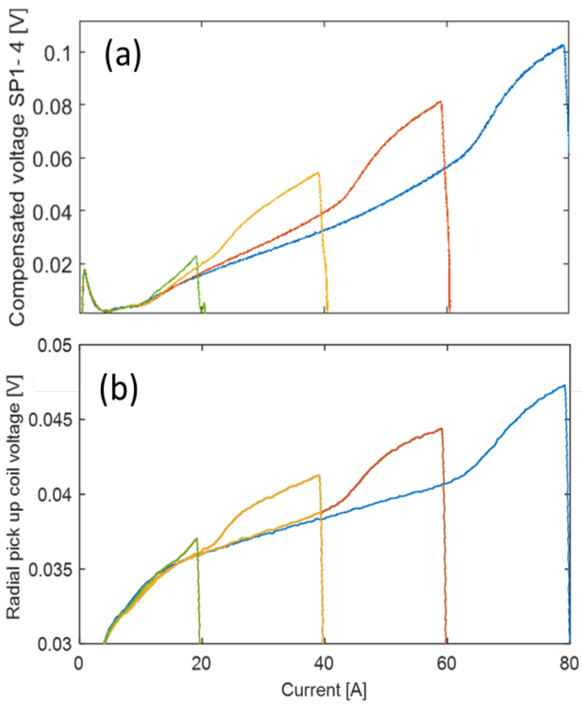

Fig. 2: Evolution of voltages during successive current ramps up to 20, 40, 60 then 80 A after initial cooling at 50 K. (a) Compensated voltage using classical axial pick up coil. (b) voltage observed on a radial pick up coil.

a simple threshold for protection purpose. This was observed during recent tests of the 20 SP coil at various temperatures, when successively ramping up the coil current to increasing targets after cooling down, as shown Fig. 2a for the compensated voltage across pancakes 1 to 4.

That hysteretic behaviour can be understood: the pick-up coil is well coupled to the REBCO coil “main” field, that is the field produced by the transport current circulating in the conductor, but do not have the same coupling with the shielding and coupling currents-induced field, whose topology is different. A correct compensation coefficient to cancel one contribution will necessarily fail to cancel the other one. In this work, an additional pick up coil was placed radially at the outer diameter, over the bottom half of the 20 pancake stack, in order to be well coupled with the shielding current induced field. The resulting pick-up coil configuration is shown Fig. 3.

The voltage over this radial pick-up coil is shown Fig. 2b to be compared to the existing compensated coil voltage Fig. 2a. The similarity in these two voltages dynamics is obvious.

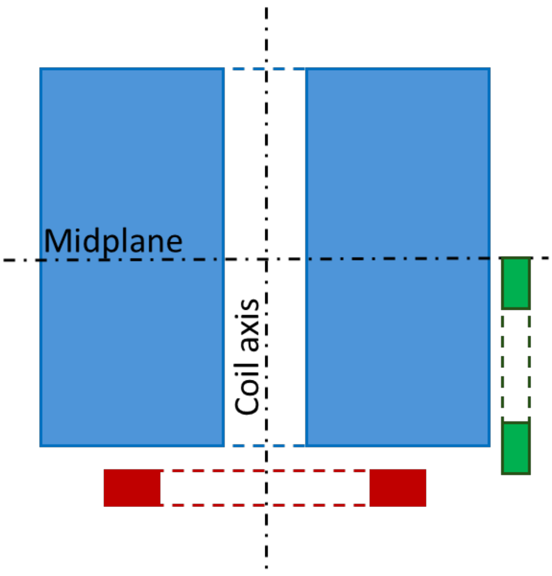

Fig. 3: Coil configuration. In blue the REBCO coil. In red the classical and already-existing pick-up coil (axial orientation). In green the additional radial pick up coil used to compensate shielding current induced field contributions.

A subtraction, performed a posteriori Fig. 4, yields a “double-compensated voltage” whose drift is much smaller, though not completely flat. The use of such double compensation would make it possible to use a simple threshold value scheme sensitive enough for quench protection of full scale REBCO insert, as the obtained signal does not vary beyond a 10 mV window.

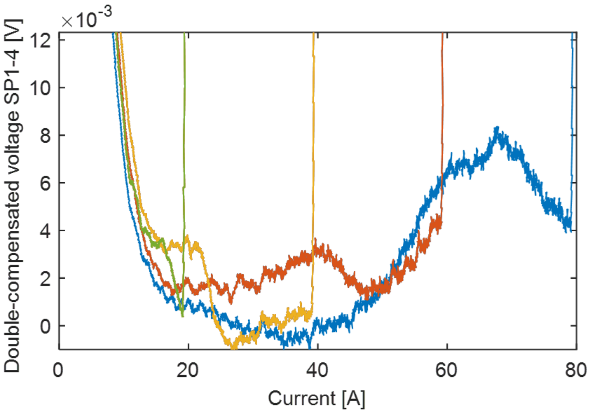

Fig. 4 Double-compensated voltage obtained by post-processed subtraction of radial pick-up coil voltage variations to the classical compensated voltage across pancakes 1 to 4 of the 20 SP REBCO coil

References

[1] S. Awaji et al., “Robust REBCO Insert Coil for Upgrade of 25 T Cryogen-Free Superconducting Magnet,” IEEE Trans. Appl. Supercond., vol. 31, no. 5, Art. no. 4300105, 2021

[2] A. Badel et al., “Detection and Protection Against Quench/Local Thermal Runaway for a 30 T Cryogen-Free Magnet,” IEEE Trans. Appl. Supercond., vol. 31, no. 5, Art. no. 4700705, 2021

[3] J. Vialle, A. Badel, B. Rozier and P. Tixador, “Transient voltages and energy balance in REBCO insulated magnet: experimental and numerical studies”, Supercond. Sci. Technol, 34(3), 115012, 2021

[4] J. Vialle, A. Badel and P. Tixador, "12 T Insulated REBCO Magnet Used as 1 MJ SMES: Protection Strategies and Preliminary Assembly Tests," IEEE Trans. Appl. Supercond., vol. 32, no. 6, Art no. 4702307, 2022

Keywords: High magnetic field, High Tc Superconductors
Arnaud Badel, CNRS Research Associate, G2Elab / Neel Institute, Grenoble, France
E-mail: Arnaud.badel@neel.cnrs.fr

TOP

Spintronic Multilayers for Energy Efficient Electronic Memory Applications

Professor Del Atkinson

This ICC Visiting Professorship at IMR, Tohoku University (Nov 2025–Jan 2026) advanced experimental research on spintronic multilayers for energy-efficient memory. Studies focused on ferromagnetic damping in CuO-based systems, revealing promising spin–orbit effects. Outcomes include ongoing collaboration, invited seminars, and a manuscript in preparation.

The primary scientific objective of the visit was to explore the materials physics underpinning applications for more energy efficient switching in spintronic/orbitronic memory technologies. A central component of the research involved experimental investigations of ferromagnetic damping in multilayer heterostructures incorporating CuO-based systems. These systems are of particular interest due to their potential to host enhanced spin–orbit and orbitronic effects, offering new pathways to manipulate angular momentum transfer with reduced power consumption.

Working closely with **Professor Seki** and collaborators at IMR, I contributed to the fabrication, measurement, and analysis of thin-film multilayers designed to probe interfacial spin transport and damping in Pt/Co/CuCuO_x. Ferromagnetic resonance techniques, FMR and ST-FMR, were employed to quantify damping parameters and to assess how CuO_x incorporation modifies damping. This could be linked to spin relaxation or orbital currents and spin–orbit coupling effects. The results obtained during the visit indicate promising trends toward tuneable damping and enhanced interfacial phenomena that could enable more energy-efficient spintronic device operation, see fig. 1. This research collaboration remains ongoing, with further experiments undertaken at IMR and analysis continuing beyond the visit. A joint manuscript is currently in development.

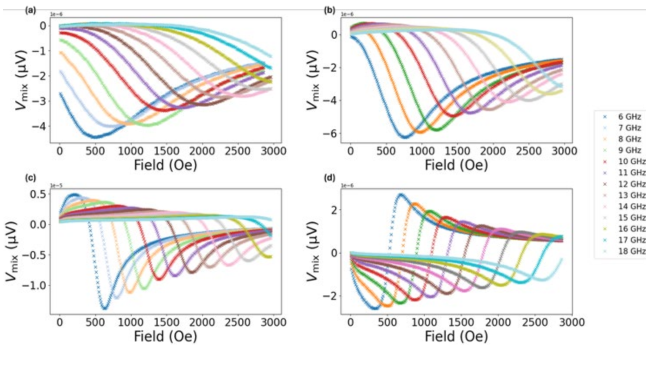

Fig 1. Spin-torque ferromagnetic resonance (ST-FMR) spectra for Pt(8 nm)|Co(3 nm)|Cu(x nm) films, for (a) x = 4, (b) x= 5, (c) x = 7, and (d) x = 10, for frequencies from 6 - 18 GHz.

In addition to experimental research, the ICC Visiting Professorship strongly supported scientific exchange and dissemination activities. I delivered a research seminar at IMR in December 2025, see fig. 2, presenting my recent work on rare-earth: transition metal alloy thin films for spintronics. I also gave invited research seminars at the National Institute for Materials Science (NIMS) in Tsukuba in January 2026 and at Kyushu University later in January 2026**.** In all external seminars, academic engagements and on LinkedIn, it was clearly stated that my visit and activities were supported by the ICC Visiting Professorship at IMR, Tohoku University.

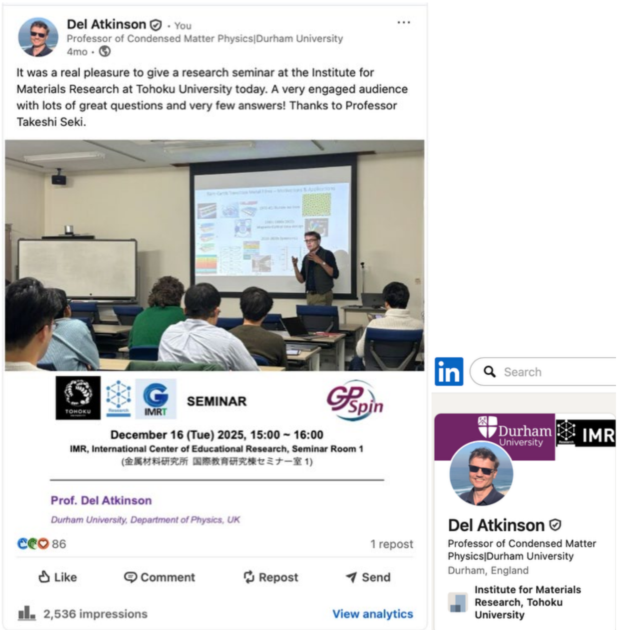

Fig2. Photo of Research Seminar at IMR posted on LinkedIn

Overall, the ICC Visiting Professorship enabled a highly productive period of experimental research, international collaboration, and academic exchange, contributing meaningfully to the development of next-generation energy-efficient spintronic memory technologies.

References

A Hodgkiss, V Kushwaha, H Suzuki, S Sakamoto, T Seki & D Atkinson - In preparation

Thermodynamic signatures of a nearby quantum critical endpoint in UTe_2 under intense magnetic field

We have performed a magnetization study of the unconventional superconductor UTe_2 under pulsed magnetic fields up to 55 T. The magnetic field was tilted by an angle θ from the direction **b** towards the direction **c** of the sample. Our measurements show that the enhancement with θ of the metamagnetic field is accompanied by a reduction of the first-order step in the magnetization, indicating the proximity of a quantum critical endpoint. In the light of our results, a next challenge will be to determine the relation between the quantum critical endpoint and the stabilization of field-induced superconductivity beyond 40 T in this system under magnetic fields tilted by a magic angle $\theta = 35°$.

Several field-induced superconducting phases have been discovered in the paramagnetic heavy-fermion compound UTe_2, revealing a new playground to study the relation between magnetism and superconductivity. At zero magnetic field, a superconducting phase SC1 below $T_{sc} \approx 2$ K was identified as a candidate for a triplet mechanism [1,2]. Under a magnetic field applied along the hard magnetic direction **b**, SC1 vanishes near 20 T and a field-induced superconducting phase SC2 is stabilized near a metamagnetic transition at $\mu_0 H_m = 34$ T, for $H \lesssim H_m$ [3,4,5]. The metamagnetic transition is associated with a first-order step $\Delta M = 0.55\ \mu_B$/U in the magnetization, which precedes the onset of a polarized paramagnetic (PPM) regime. By tilting the magnetic field by a magic angle $\theta = 35°$ from **b** to **c**, a second field-induced superconducting phase SC-PPM is stabilized for $H \gtrsim H_m$, i.e., in the PPM regime beyond the metamagnetic transition observed then at $\mu_0 H_m = 40 - 45$ T [5,6].

Figure 1 shows that the amplitude of the step ΔM induced in the magnetization at the metamagnetic field, decreases when the

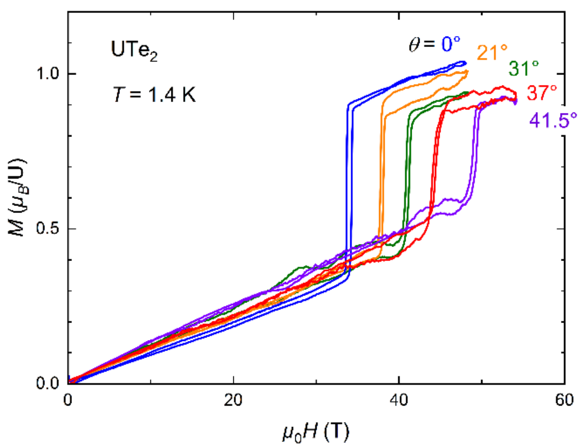

Figure 1: Magnetization versus magnetic field of UTe_2, measured under magnetic-field directions tilted by different angles θ from **b** to **c** at the temperature $T = 1.4$ K.

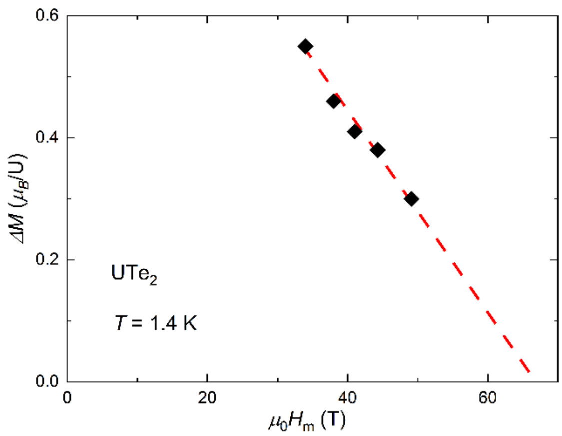

Figure 2: Step ΔM in the magnetization at H_m versus H_m measured in UTe2 under magnetic-field directions tilted by different angles θ from **b** to **c** at the temperature $T = 1.4$ K.

metamagnetic field is increased by tilting its direction by an angle θ from **b** to **c**. For $\theta = 41°$, $\Delta M = 0.3\ \mu_B$/U has been reduced by a factor 2 in comparison with its value for $\theta = 0°$. As shown in Figure 2, ΔM is linearly related to H_m. Assuming that this linear relation can be extrapolated at larger angles θ, our ΔM versus H_m data indicate the possible presence of a quantum critical endpoint, at which the first order character of the metamagnetic transition would vanish, for a critical value of the metamagnetic field $\mu_0 H_m^c = 65 - 70$ T. Our results raise several questions. What is the relation between the field-induced superconducting phases and the possible presence of a quantum critical endpoint of the metamagnetic transition? Can we observe other field-induced superconducting phase (s) at larger magnetic fields and beyond the quantum critical endpoint? To answer these questions, new series of magnetization experiments, under wider ranges of temperatures and magnetic fields will be needed.

This work was done in collaboration with S.

Kalaiarasan from the LNCMI-Toulouse, A. Miyake and D. Aoki from the IMR Oarai at the Tohoku University, and M. Kondo and M. Tokunaga from the ISSP Kashiwa.

References

[1] S. Ran, C. Eckberg, Q.-P. Ding, Y. Furukawa, T. Metz, S. R. Saha, I.-L. Liu, M. Zic, H. Kim, J. Paglione, and N. P. Butch, Science 365, 684 (2019).
[2] D. Aoki, A. Nakamura, F. Honda, D. Li, Y. Homma, Y. Shimizu, Y. J. Sato, G. Knebel, J.-P. Brison, A. Pourret, D. Braithwaite, G. Lapertot, Q. Niu, M. Valiska, H. Harima, and J. Flouquet, J. Phys. Soc. Jpn. 88, 043702 (2019).
[3] A. Miyake, Y. Shimizu, Y. J. Sato, D. Li, A. Nakamura, Y. Homma, F. Honda, J. Flouquet, M. Tokunaga, and D. Aoki, J. Phys. Soc. Jpn. 88, 063706 (2019).
[4] G. Knebel, W. Knafo, A. Pourret, Q. Niu, M. Valiska, D. Braithwaite, G. Lapertot, M. Nardone, A. Zitouni, S. Mishra, I. Sheikin, G. Seyfarth, J.-P. Brison, D. Aoki, and J. Flouquet, J. Phys. Soc. Jpn. 88, 063707 (2019).
[5] S. Ran, I.-L. Liu, Y. S. Eo, D. J. Campbell, P. Neves, W. T. Fuhrman, S. R. Saha, C. Eckberg, H. Kim, J. Paglione, D. Graf, J. Singleton, and N. P. Butch, Nat. Phys. 15, 1250 (2019).
[6] W. Knafo, M. Nardone, M. Valiska, A. Zitouni, G. Lapertot, D. Aoki, G. Knebel, and D. Braithwaite, Commun. Phys. 4, 40 (2021).

Keywords: Unconventional Superconductivity, Metamagnetism, High Magnetic Field
William Knafo (LNCMI-Toulouse)
E-mail: william.knafo@lncmi.cnrs.fr

Accepted No.	Title・Applicant・Affiliation	Host	Proposed Research	Term
25FS1	Ph.D. Student Seetharaman Senthamizh Raja・Anna University, India	Prof. Fujiwara	In-Situ Observation of Growth Process of InSb and InGaSb Semiconductor Crystals for Thermoelectric Application	2025.5.18-2025.8.17
25FS2	Dr. Karol Andrzej Bartosiewicz・Institute of Physics of the Czech Academy of Sciences, Czech	Prof. Yoshikawa	Multi-Site Lattice Engineering in Fe^{3+}- and C^{3+}-Doped Eutectic Crystals: A Systematic Approach to High-Power Broadband NIR-LED Light Source Applications	2025.9.15-2025.12.12
25FS3	Ph.D. Student Lipika・Indian Institute of Technology Delhi, India	Prof. Umetsu	Investigating the Interplay of Real Space and Momentum Space Berry Curvature on the Physical Properties of Quantum Magnets	2025.10.2-2025.12.2
25FS4	Ph.D. Student Yang Yuyan ・Shanghai University	Prof. Yamanaka	SEBM 3D Printing Microstructure Regulation of Fe-Cr-Mo System Amorphous Alloys Based on Machine Learning and Melt Pool Characterization	2025.12.6-2026.3.3
25FS5	Ph.D. Student Tarun Pratap Singh・Guru Ghasidas Vishwavidyalaya, Bilaspur, India	Prof. Nojiri	High Magnetic Field Magnetization and Phase Transitions Studies in $A_2M_{o3}O_8$ (A = Fe, Mn) Polar Magnetic Systems	2025.10.12-2025.12.14
25FS6	Ph.D. Student Haribrahma Singh・Indian Institute of Technology Delhi, India	Prof. Umetsu	Unveiling Exotic Quantum Phenomena in Ternary Metal Pnictide-Based Intermetallics: Probing Topological States through Quantum Oscillations	2025.8.1-2025.10.25
25FS7	Ph.D. Student David Gracia・University of Zaragoza, Spain	Prof. Nojiri	High Magnetic Field Heat Capacity on Fe-Based Molecular Magnets	2026.1.4-2026.3.1

TOP

In-situ observation of InSb and InGaSb crystal-melt interface and analysis of dendrite formations

Abstract:-- In this study, the effect of gradient freezing and grain boundary distribution on the formation of dendritic structures of InSb and InGaSb were analysed. The growth process of pure InSb and $In_{1-x}Ga_xSb$ alloy semiconductors were in-situ observed. The materials were crystallized under pre-determined cooling rates. The growth process was monitored and recorded using a microscope with video recorder. The growth rates of crystals were analysed from the t-x plot. The grain structures of the grown crystals were analysed after the in-situ experiments.

In-situ observation of crystallization process gives us deep insights about determination of microstructures, such as grain size, crystal orientation and some defect formations like twins and dendrites. This experimental investigation helps to understand how the polycrystalline semiconductor crystals are formed during melt growth.

The high purity source materials of In & Sb (99.99%) were cleaned by ultrasonication in acetone, etched in dil.HNO_3(HNO_3:H_2O=1:1) for 5 minutes and rinsed in distilled water followed by drying using N_2 gun. InSb ingots were prepared by melting In and Sb granules in a vacuum sealed quartz ampoule at 700°C and cooling to RT slowly for 24h (28°C/h). The prepared ingots were cleaned by etching the surface using HF : HNO_3 : CH_3COOH in 2:5:4 ratio. The crystallization of InSb from melt was in-situ observed at different cooling rates of 5, 10, 15, 30 K/min using specially designed furnace in which two independently controlled heaters were engaged to establish a temperature gradient of 6K/mm. The crystallization process was monitored and recorded using Keyence VHX-600 microscope. The grain structures of InSb ingots solidified at different cooling rates were analysed by Electron Backscatter Diffraction pattern (EBSP) using JEOL JSM-6610A. Similar procedure was followed for in-situ observing the crystallization process of $In_{1-x}Ga_xSb$.

During the in-situ observation of InSb, a thin layer of oxide layer was formed on the melt surface which makes it difficult to observe the growth process. Hence a thin quartz plate was placed on top of the crucible to avoid the oxide layer formation and the growth of InSb was in-situ observed [1]. At low cooling rates (< 15 K/min) no dendrites were formed on the InSb melt surface. At the higher cooling rate of 30 K/min, dendrites were formed with clear facets (Fig.1) and the dendrites were emerged from the facets of the grooves which were initially formed by the twin boundaries and led to faster growth as a result of twin plane re-entrant edge mechanism. The re-entrant corner created by the twins acted as a step source due to which continuous and faster growth was observed from its core. The growth behaviour of the crystal-melt interface with grooves and dendrites were analysed by t-x plot and in relation with change in growth rate as a function of time with isochrones. The grain structures and orientations of the grains around the dendritic structures were examined using EBSP analysis. During the experiments with the ternary $In_{1-x}Ga_xSb$ system, the vigorous oxidation and expansion on the surface of the ingot made it difficult to be observed through the microscope.

Furthermore, the results of the growth behaviour analysis will be compared with theoretical models and will be validated. The outcomes of the experiments paves way for designing an optimized growth conditions that leads to the growth of defect controlled InSb crystals. Such ingots can be used in various applications like IR sensing, photovoltaics, thermoelectrics and so on.

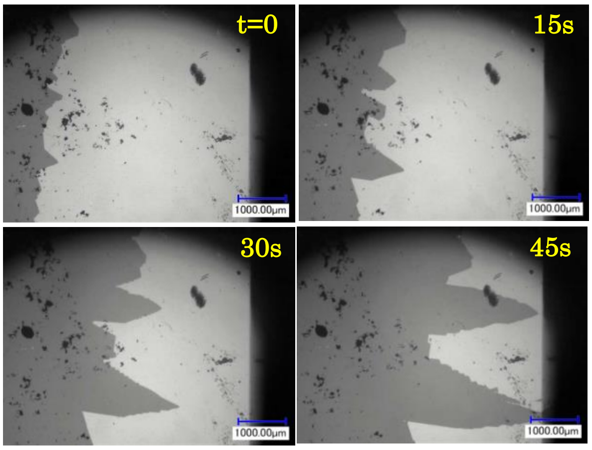

Fig.1 Faceted dendrites grown at crystal-melt interface.

References

[1] Shiga, K., Takahashi, A., Chuang, L.C., Maeda, K., Morito, H. and Fujiwara, K., 2022. Journal of Crystal Growth, 577, p.126403.

Keywords: directional solidification, dendrites, grain boundaries
Seetharaman Senthamizh Raja (Centre for Nanoscience and Technology, Anna University, INDIA)
E-mail: senthamizhrajas@gmail.com

Stabilization of Cr^{4+} near-infrared luminescence through eutectic crystal engineering

Eutectic microstructures provided an effective strategy for tuning luminescence through phase coupling. The $Y_3Al_5O_{12}$–$YAlO_3$:Cr,Mg eutectic crystal grown by the micro-pulling-down method exhibited a well-defined lamellar microstructure, markedly broadened Cr^{4+} R-line emission and exclusively Cr^{4+} luminescence. By contrast, the uPD-grown $Y_3Al_5O_{12}$:Cr,Mg single crystal was phase-pure garnet and showed well-resolved Cr^{4+} R-lines together with concurrent Cr^{3+} and Cr^{4+} emissions. These findings established phase-coupled eutectics as an effective approach for tailoring Cr-based functional materials.

Broadband Cr^{4+} luminescence is attractive for near-infrared (NIR) photonics, yet its stabilization, efficiency and local-site control remain poorly understood [1]. We investigated whether eutectic phase coupling in the Cr,Mg-doped $Y_3Al_5O_{12}$–$YAlO_3$ (YAG–YAP:Cr,Mg) system could promote Cr^{4+} stabilization and enable optical functionality inaccessible in conventional $Y_3Al_5O_{12}$:Cr,Mg (YAG:Cr,Mg) single crystals [2]. Fig.1A shows photographs of the as-grown YAG:Cr,Mg single and YAG–YAP:Cr,Mg eutectic crystals. The dark brown color of both samples indicated a dominant fraction of Cr^{4+} ions [3]. SEM–EDS mapping (Fig. 1B) reveals high elemental homogeneity in the single-crystal and well-defined lamellar eutectic microstructure in the composite. Powder XRD (Fig. 1C and 1D) confirms phase-pure garnet YAG in the single crystal and the coexistence of YAG and YAP in the eutectic

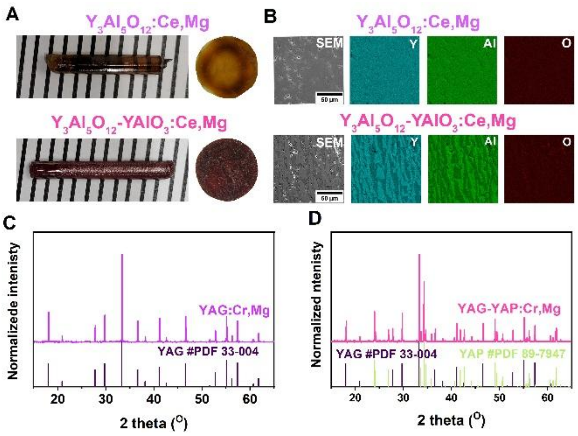

Fig. 1 (A) Photographs of the as-grown YAG:Cr,Mg single crystal (top) and YAG–YAP:Cr,Mg eutectic crystal (bottom), together with polished plates. (B) SEM micrographs and EDS elemental maps (Y, Al and O). Powder XRD patterns of (C) YAG:Cr,Mg and (D) YAG–YAP:Cr,Mg crystals.

Figure 2a shows the characteristic Cr^{4+} absorption bands in YAG:Cr, whose strong absorption in the visible range accounted for the brown coloration [3]. Under 980 nm excitation, both YAG:Cr and YAG–YAP:Cr exhibited broad near-infrared Cr^{4+} emission, whereas the eutectic

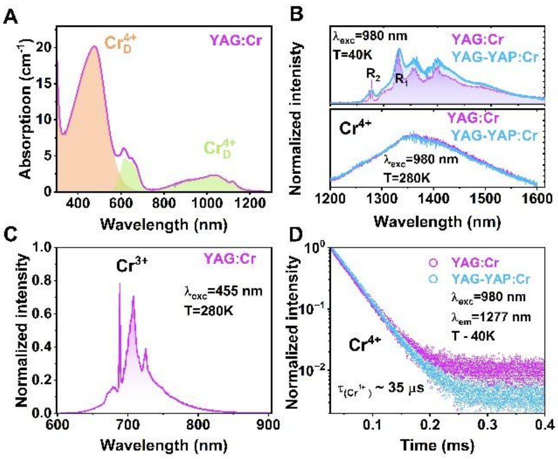

Fig. 2 (A) RT absorption spectrum of YAG:Cr showing Cr^{4+} bands. (B) Cr^{4+} emission spectra of YAG:Cr and YAG–YAP:Cr under 980 nm excitation at 40 and 280 K. (C) Cr^{4+} emission spectrum of YAG:Cr at 280 K under 455 nm excitation. (D) Cr^{4+} emission decay of YAG:Cr and YAG–YAP:Cr at 40 K (λ_{exc}=980 nm, λ_{em}=1277 nm).

shows broader low-temperature R-line emission (Fig. 2B), consistent with a broader distribution of local crystal fields. By contrast, Cr^{3+} emission was observed exclusively in YAG:Cr under 455 nm excitation (Fig. 2C). Time resolved measurements revealed similar Cr^{4+} decay kinetics in both samples, with a lifetime of ~35 μs at 40 K (Fig. 2D). These results show that eutectic phase coupling broadened the Cr^{4+} R-line emission and enabled complete conversion of Cr^{3+} to Cr^{4+}. Eutectic engineering therefore emerged as a promising strategy for achieving exclusively Cr^{4+} luminescence for advanced photonic applications.

Acknowledgment

This work was supported by ICC-IMR, Tohoku University.

References

[1] M. Chaika et al., J. Eur. Ceram. Soc. 44, 7432–7450 (2024).
[2] R. Feldman et al., Opt. Mater. 24, 333–344 (2003).

Keywords: crystal growth, luminescence, infrared (ir) spectroscopy
Full Name: Dr Karol Andrzej Bartosiewicz, Institute of Physics of the Czech Academy of Sciences, Prague, Czechia
E-mail: bartosiewicz@fzu.cz
http://p4f.fzu.cz/fzu_fellow/karol-bartosiewicz-ph-d/

Investigating the interplay of real space and momentum space Berry curvature on the physical properties of Quantum magnets

Lipika[1], Rie Umetsu[2], Kaustuv Manna[1]

[1]Department of Physics, Indian Institute of Technology, Delhi, India

[2]Cooperative Research and Development Centre for Advanced Materials, IMR, Tohoku University

First, we carried out electrical transport studies to uncover the effect of Ba substitution at the Eu site in topological semimetal EuAuBi and, correspondingly, understand how substitution can be an effective means to control the spin textures in this system. Secondly, we performed transport measurements on distorted Kagome material $Tb_6Ti_4Al_{43}$ to uncover the intrinsic properties of this system.

The real-space magnetic spin textures have been experimentally observed in Dirac semimetal EuAuBi [1]. Prior theoretical studies predict that the partial substitution of Eu with Ba in EuAuBi can modify the long-range magnetic interactions and can drive a transition between Dirac semimetal and Weyl Semimetal. This establishes elemental substitution as an effective tuning parameter for controlling the interplay between magnetism and band topology [2]. Motivated by this, we aimed to understand its effect on the real-space magnetic textures observed in EuAuBi. Since magnetic structure directly governs both real-space and momentum-space Berry curvature, in such systems, tuning magnetic interactions via Ba doping provides a pathway to manipulate emergent spin textures and their associated transport signatures. With increasing Ba concentration, a decrease in the hysteresis feature is observed, consistent with the dilution of magnetic Eu^{2+} interactions by non-magnetic Ba. However, at 15% substitution, hysteresis with magnitude comparable to pristine EuAuBi is observed, which is again suppressed at higher substitution indicating a non-monotonic evolution of magnetic correlations. To further probe the evolution of spin textures, Hall measurements were performed to extract the changes in the topological Hall effect (THE), which can serve as a sensitive tool to probe real-space Berry curvature. For, $Eu_{0.95}Ba_{0.05}AuBi$ and $Eu_{0.90}Ba_{0.10}AuBi$, a negative THE is observed, which is contrary to positive THE in EuAuBi. Nevertheless, the sign reversal of THE points indicates the presence of spin textures with opposite chirality compared to the parent compound. In conclusion, this study demonstrates that Ba substitution acts as a tuning parameter for controlling real-space spin textures in the system.

$Tb_6Ti_4Al_{43}$: The crystal exhibits the antiferromagnetic ground ordering with $T_N \sim 20$ K. For a magnetic field applied along the c-axis (B // c), a strong metamagnetic switching is observed, accompanied by clear asymmetric hysteresis at low temperatures, whereas for a field applied along the ab plane, the spin-flop transition is observed. Additionally, the metamagnetic transition is strongly reflected in magneto transport measurements, giving rise to pronounced anomalies in magnetoresistance and an anomalous Hall contribution, despite the ground state of the system being antiferromagnetic. Our results highlight the interplay of geometrical frustration, anisotropic magnetic interactions, and spin–charge coupling in a distorted Kagome antiferromagnet, establishing Tb6Ti4Al43 as a promising platform for studying field-induced magnetic phase transitions in frustrated systems.

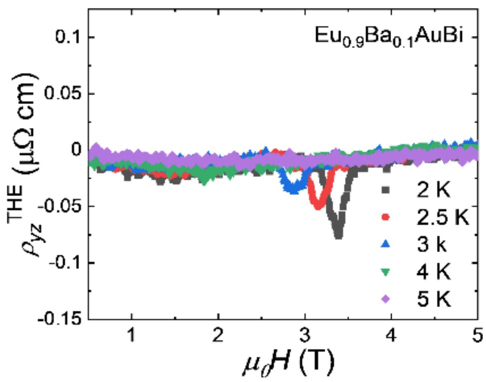

Figure 1: Fig shows the negative topological Hall effect in 10% Ba substituted EuAuBi.

References

1) Lipika, S. Singh, A. Saraswati, et al., Phys. Rev. B 2026,**113**, 104406

2) Y.Du, B.Wan, D. Wang, et al, Sci Rep 2015,5:14423

Keywords: magnetism, magnetoresistance, Hall effect
Full Name: Indian Institute of Technology, Delhi
E-mail: lipika@physics.iitd.ac.in

SEBM microstructure regulation of Fe-Cr-Mo amorphous alloys based on melt pool characterization

Introductory part, Abstract: Fabricating large-scale Fe-based bulk metallic glasses via electron beam additive manufacturing (EBM) is challenged by uncontrolled crystallization. This study investigates the process for $Fe_{55}Cr_{25}Mo_{16}B_2C_2$ using experiments and simulation. Results show substrate segregation affects melt pool homogeneity, and a quantitative correlation exists between parameters and pool geometry. Simulations identify a critical cooling rate (~10^3 K/s) for amorphous formation. Marangoni convection transports Mo/Cr, delaying homogenization and retarding amorphous formation by 15-20%. These findings provide a basis for tailoring EBM parameters.

Electron beam additive manufacturing (EBM) offers a promising route to fabricate large-scale Fe-based bulk metallic glasses (BMGs), yet crystallization control remains a key challenge . This work focuses on the $Fe_{55}Cr_{25}Mo_{16}B_2C_2$ alloy[1][2][3][4].

Fig.1 shows the substrate, prepared by spark plasma sintering, exhibited significant Cr segregation which persisted into the melt pool. Single-track experiments established clear quantitative relationships between process parameters (beam current, scan speed) and melt pool dimensions .

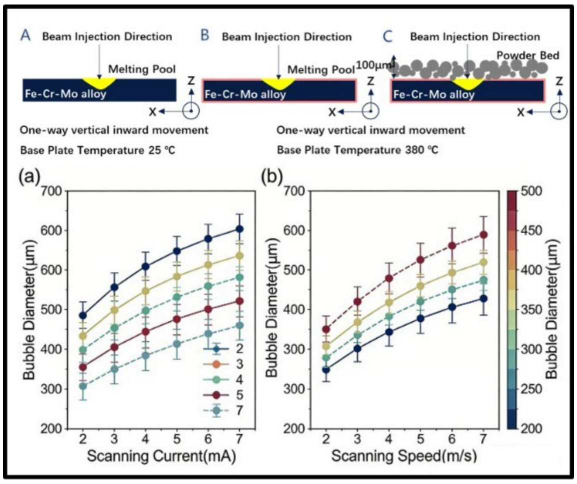

Fig. 1 The Relationship Between Melt Pool Geometry and Parameters

Fig. 2 showed the amorphous microstructural characterization which revealed that a critical cooling rate on the order of 10^3 K/s is required for amorphous phase formation, with the pool center being more favorable. However, intense Marangoni convection within the melt pool preferentially transports Mo and Cr elements towards the pool rear.

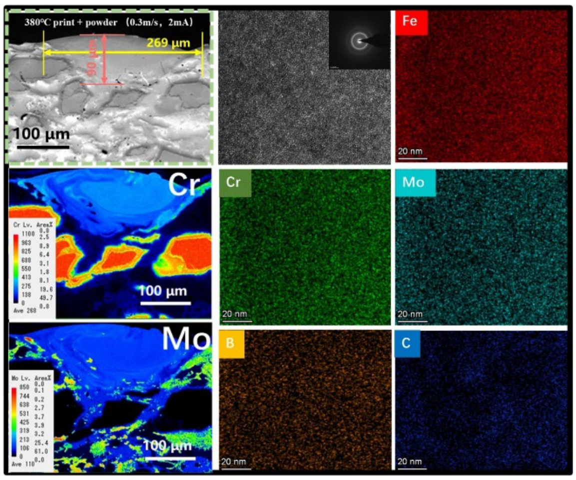

Fig. 2 Characterization of the microstructure and compositional distribution of the melt pool

Consequently, a strategic balance between achieving high cooling rates and minimizing convective solute disturbance is crucial for maximizing the amorphous fraction.

This solute transport delays compositional homogenization and retards amorphous phase formation in the central region by an estimated 15-20% compared to static conditions. The study elucidates the coupled thermal-fluid-solute mechanisms governing crystallization during EBM, providing a quantitative basis for process optimization to achieve high-performance, bulk amorphous components.

References

[1] Inoue A., Takeuchi A., MATER. TRANS. 46, 22-39 (2005)
[2] Wang W. H., Dong C., Shek C. H., Mater. Sci. Eng. R Rep. 44, 194-207 (2004)
[3] Galati M., Lanzetta M., Addit. Manuf. 41, 198324 (2021)
[4] Galati M., Iuliano L. , Addit. Manuf. 23, 123889 (2018)

Keywords: amorphous, microstructure,powder metallurgy
Full Name Yuyan Yang (Materials Genome Institute, Shanghai University, Shanghai, 200444, PR China)
E-mail: yyyqwerty@126.com

High Magnetic Field Magnetization and Phase Transitions Studies in $A_2Mo_3O_8$ (A = Fe, Mn) Polar Magnetic Systems

Brief Introduction:

Multiferroic systems are very promising for low power memory devices in recent days. Among these multiferroics, Type –III multiferroics have collinear magnetic structure rather than complex structure where polarization are in built, driven by chemical ordering, show large change in polarization at transition temperature and hence strong ME coupling. The polar magnets family $A_2Mo_3O_8$ (A: divalent transition metal ion) having hexagonal crystal structure, crystallizes in space group *P6₃mc* is recently considered as type-III multiferroics being studied in recent times due to the promising magneto-electric (ME) enhancement and tuning magnetic properties by playing with the substitution of magnetic ions with different transition metal ions at A-site. The isostructural compound $A_2Mo_3O_8$ are very interesting due to having different magnetic ground states. $Fe_2Mo_3O_8$ and $Mn_2Mo_3O_8$ exhibit antiferromagnetic (AFM) and ferrimagnetic (FIM) ordering at 60K and 40K, respectively, with strong anisotropy along polar c-axis whereas $Co_2Mo_3O_8$ show AFM order and $Ni_2Mo_3O_8$ has unique zigzag/stripy type AFM order. Recently large ME effect was observed in $Fe_2Mo_3O_8$ and it was also demonstrated that the ME effect can be tuned to large extent by doping with non-magnetic Zn or Mg ion at Fe site and with magnetic Fe ion at Mn-site to realize linear ME effect on these compounds which leads to the enhanced ME coefficient. Recently, the metamagnetic transition or spin reorientation transition from AFM to FIM and FIM to spin-flop (SF) state were observed in parent/Zn-doped $Fe_2Mo_3O_8$ and Fe-doepd $Mn_2Mo_3O_8$, respectively at moderate magnetic field in magnetization (M-T) and polarization (P-H) measurements [1-2]. In addition, the high magnetic field (HMF) studies upto 66T, were done to realize the fully spin polarized state and multistage ME states with the multistep behavior correspond metamagnetic transition through M-T and P-H measurements in $Fe_2Mo_3O_8$ [3] which will possibly pave the path to design low power consumption multistage ME devices. The polar magnets $Mn_2Mo_3O_8$ though exhibits the transition from FIM to SF state at moderate applied field at 2K, the fully spin polarized state were not realized from best of our knowledge present in the literature and may be observed in HMF measurements in this compound. It is imminent to think that the HMF properties such as distinct multistage ME states and rich magnetic phases can be explored via HMF measurements in $Mn_{2-x}Ni_xMo_3O_8$ and $Fe_{2-x}Co_xMo_3O_8$ compound to elucidate the intermediate metamagnetic transition and electric polarization.

Measurements carried out at IMR

Magnetization measurements on Pulsed field setup in $Mn_{2-x}Ni_xMo_3O_8$ compounds

We have carried out high field dependent magnetization measurements under pulsed field on $Mn_{2-x}Ni_xMo_3O_8$ (x = 0., 0.5, 0.75) and in $Fe_{2-x}Ni_xMo_3O_8$ (x =0, 0.1, 0.2) up to field limit of 30 T. All measured data is depicted in Fig 1. Figure 1(a) show a clear cusp around 4-6 T for x = 0

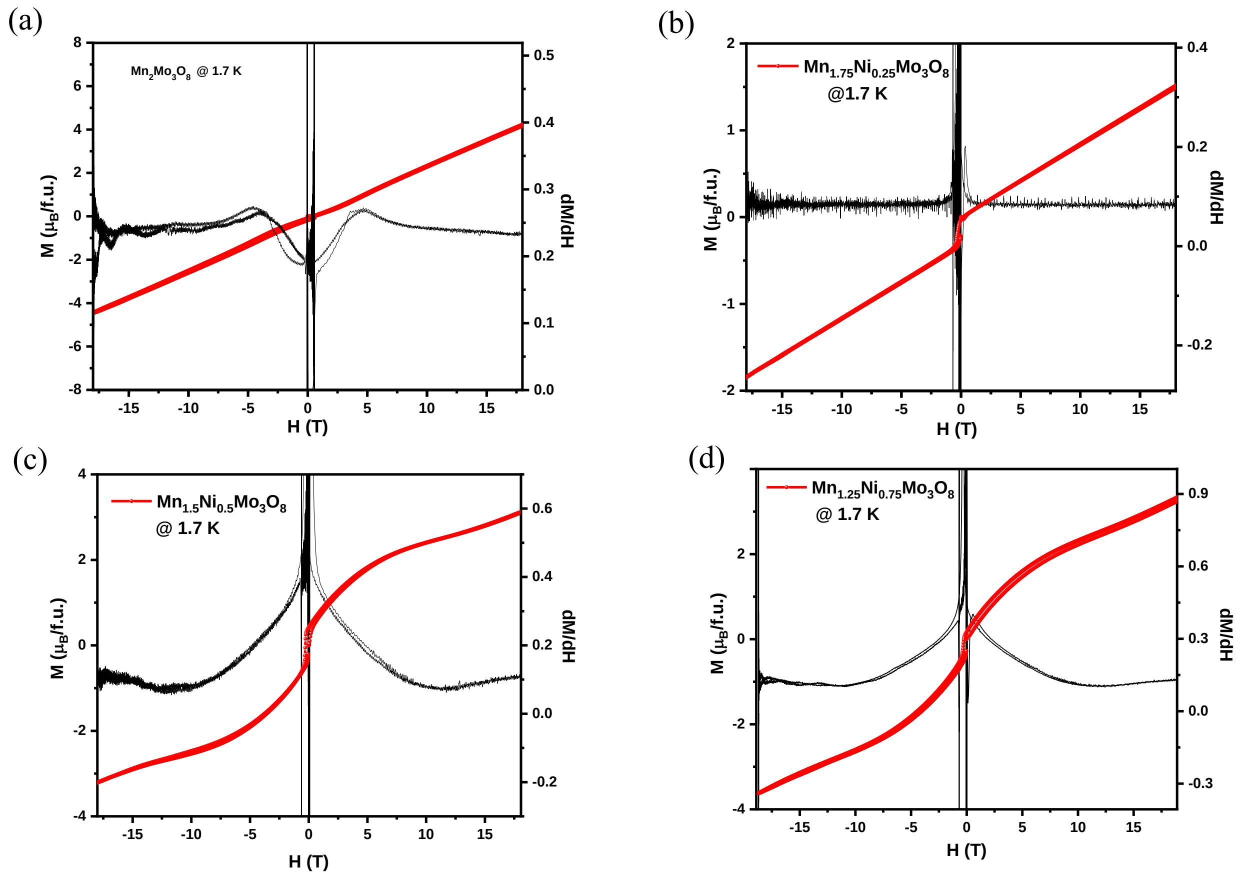

Figure 1. Field dependent magnetization measurements under pulsed magnet of field limit of 30 T on polycrystalline compounds $Mn_{2-x}Ni_xMo_3O_8$ (a) x =0, (b) x =0.25, (c) x = 0.5, and (d) x = 0.75.

shows a clear spin reorientation transition (SRT) which is well known for $Mn_2Mo_3O_8$ compound. In addition, no further spin reorientation is observed for this compound up to 30 T. For x = 0.25, compound show and small ferrimagnetic behavior at 1.7 K also rules out the possibility of SRT. Furthermore, small ferromagnetic/ ferrimagnetic establishment remained for x = 0.5 and x = 0.75 and also shows deviation from in the M vs H plot.

Polarization measurements on Pulsed field setup in $Mn_2Mo_3O_8$ single crystal

In this section we have carried out the pulsed field dependent polarization measurements on single crystal of $Mn_2Mo_3O_8$ in H// c configuration. Measurements were done at represented temperatures: 4.2 K, 12 K, 33 K and 40 K as shown in Fig. 2. The spin flop phase were appeared at 4-6 T field window at specific temperatures viz. 4.2 K, and 13 K. Above these temperature, spin flop phase vanishes off. In general, the electric polarization as a function of field is expressed by $\Delta P = P_0 + \alpha H + \beta H^2$, where P_0 represents the difference of P(H) and P(H = 0) in the same magnetic phase and usually is zero. When a magnetic field-induced metamagnetic transition occurs, P0 is the difference of P(H = 0) between the two different magnetic phases The obtained data of polarization as a function of field are fitted via above equation. The linear magnetoelelctric effect (ME) dominates in low field and low temperature region. High field and region is dominated by second order ME effect. Spin flop phase are characterized by the linear and quadratic ME effect. The ferrimagnetic state dominates foe linear ME effect in $Mn_2Mo_3O_8$ system which is governed by the exchange striction mechanism. Also, when system achieved spin flop state, spin remains collinear, rules out the Dzyaloshinskii-Moriya Interaction (DMI) in spin flop state and exchange striction again governed at this phase.

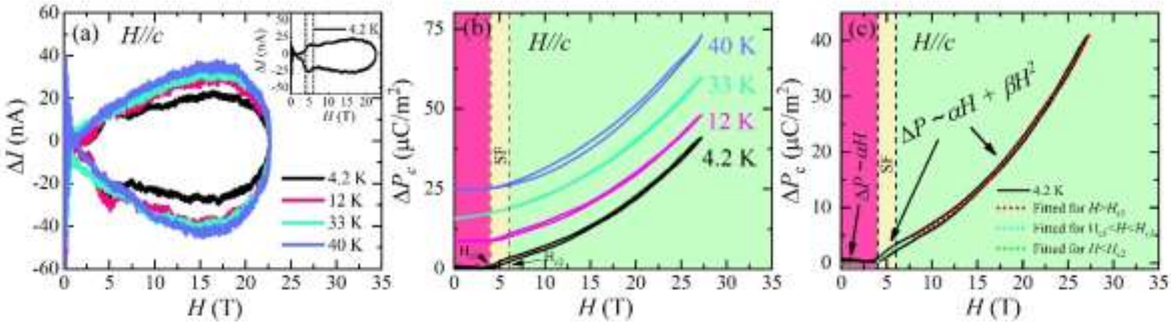

Figure 2. Field dependent polarization measurements under pulsed magnet of field limit of 30 T on single crystal of $Mn_2Mo_3O_8$ at various temperatures. (a) represents the magneto-current (b) and time integration of magneto-current gives rise the polarization and (c) fitted polarization curve at 4.2 K

Polarization measurements on different configuration viz. H//H1, H//H2 and H//H3

Further, polarization is deduced in different measurement configuration as shown in Fig. 3

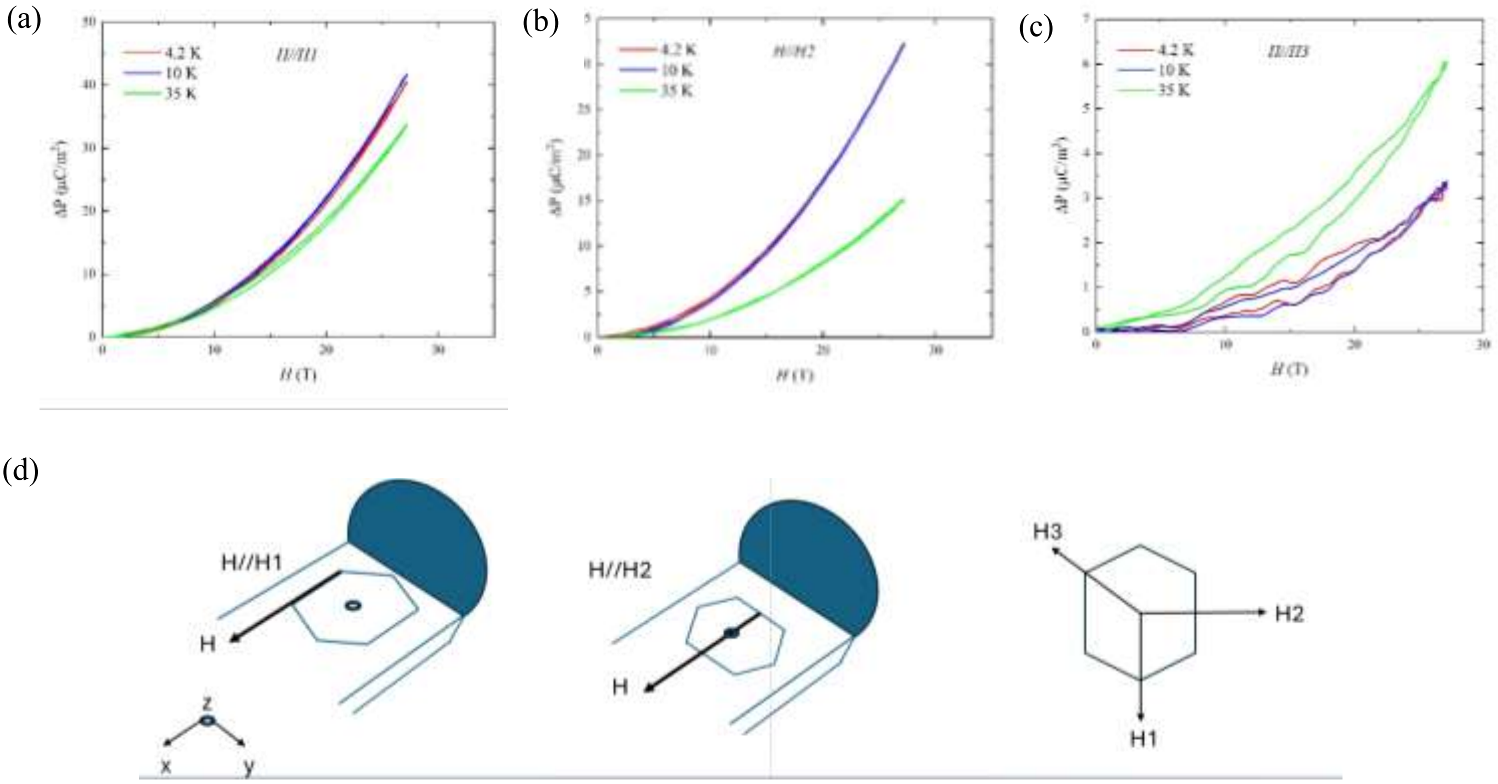

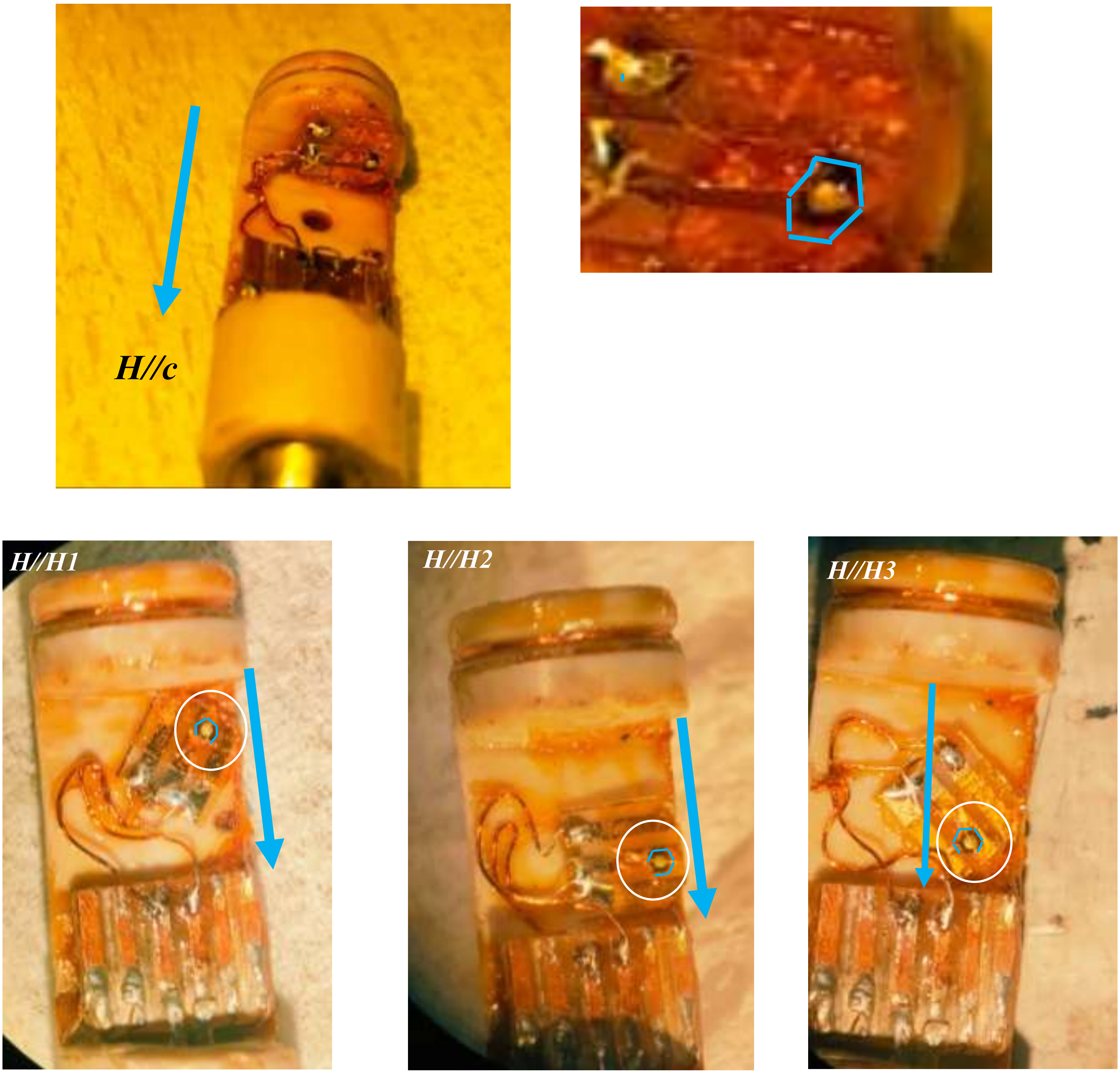

Figure 3. Field dependent polarization measurements under pulsed magnet of field limit of 30 T on single crystal of $Mn_2Mo_3O_8$ at various temperatures in different configuration. (a) H//H1 (b) H//H2 and (c) H//H3 , where H$\perp$c in all cases. (d) All measured configuration are shown.

Electron spin resonance spectroscopic studies on polycrystalline $Mn_{2-x}Ni_xMo_3O_8$ (x = 0, 0.75)

The temperature dependent electron spin resonance (ESR) under pulsed field at various frequencies were measured on polycrystalline Mn2Mo3O8. These measurements yield the gapped magnon below ferrimagnetic ordering i.e. T_C = 40 K. The splitting in the antiferromagnetic resonance (AFMR) mode below T_C = 40 K were observed due to presence of small anisotropy in the polycrystalline sample. This was further analyzed by the uniaxial AFMR theory and extracted gapped magnon frequencies for both spin excitation modes w01 = 135.67 GHz and w02 = 78.97 GHz. Furthermore, the anisotropy field from the both spin excitation modes reveal the dominance of the two coupled distinct Mn site which validates the M1 mode dominated by octahedral site while tetrahedral site is dominated by M2 mode.

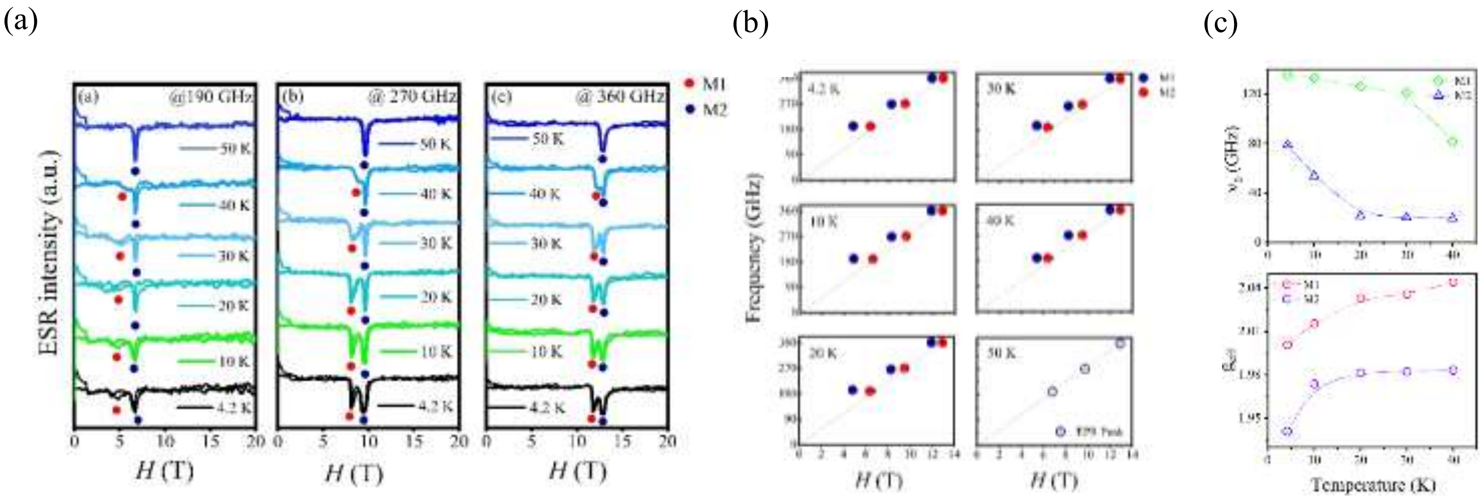

Figure 4. (a) High-field ESR spectra of $Mn_2Mo_3O_8$ system carried out at various temperature and different frequencies. (b) Frequency-field diagram to estimate gapped magnon frequency. (c) Thermal variation of gapped magnon frequency and effective *g*-values below transition temperature T_C = 40 K.

Additionally, the temperature dependent electron spin resonance (ESR) under pulsed field at various frequencies were measured on polycrystalline $Mn_{1.25}Ni_{0.75}Mo_3O_8$. These measurements yield the gapped magnon below magnetic ordering i.e. T_C ~27 K. The splitting in the antiferromagnetic resonance (AFMR) mode below T_C ~27 K were observed due to presence of small anisotropy in the polycrystalline sample. These obtained data are being analyzed for further establishments.

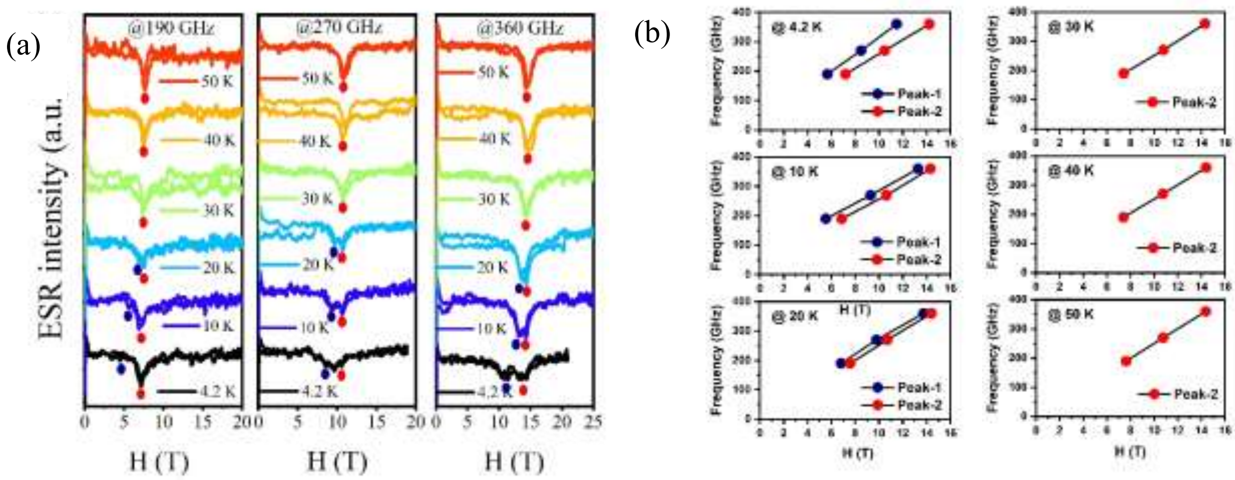

Figure 5. (a) High-field ESR spectra of $Mn_{1.25}Ni_{0.75}Mo_3O_8$ system carried out at various temperature and different frequencies. (b) Frequency-field diagram to estimate magnon gap.

Magnetization measurements on Pulsed field setup in $Fe_{2-x}Co_xMo_3O_8$ (x = 0, 0.1, 0.2) compounds

We have carried out high field dependent magnetization measurements under pulsed field polycrystalline $Fe_{2-x}Co_xMo_3O_8$ (x =0, 0.1, 0.2) compounds up to field limit of 30 T. All measured data is depicted in Fig 6. Figure 6 (a) show a monotonous linear increment on increasing field showing the antiferromagnetic ordering is robust at high field for x = 0. Some distinct features are observed for x = 0.1 and x = 0.2 compounds, where M vs H curves show some anomalous behavior, at low field region, magnetization increase linearly and around 10 T, the nonlinear behavior discernible showing the addition short range ordering or a spin reorientation for these compounds.

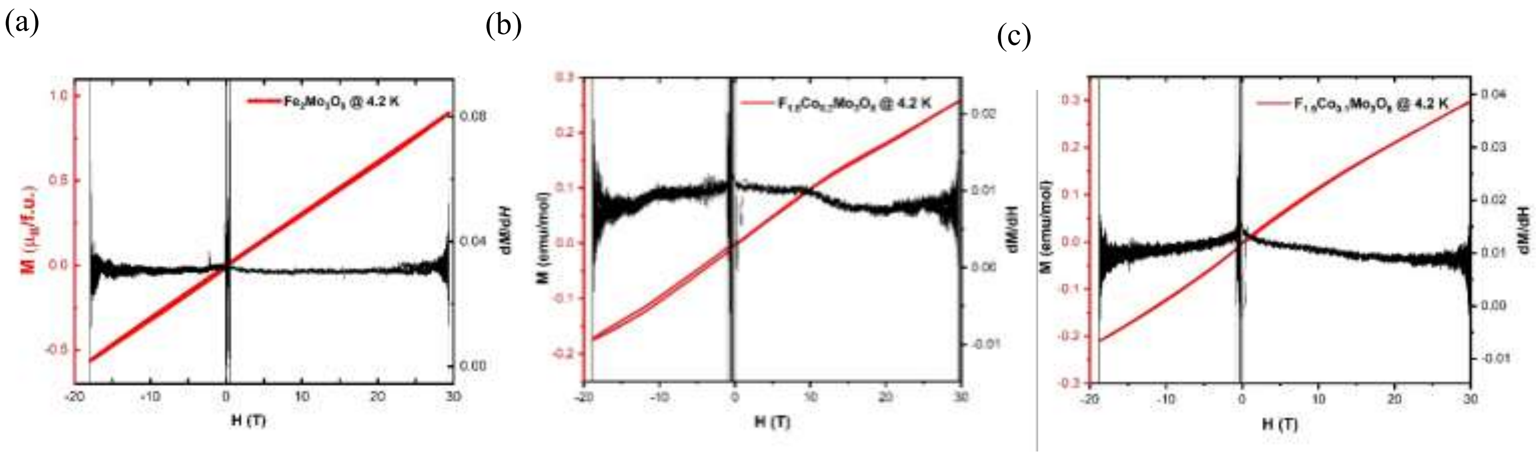

Figure 6. Field dependent magnetization measurements under pulsed magnet of field limit of 30 T on polycrystalline compounds $Fe_{2-x}Co_xMo_3O_8$ (a) x =0, (b) x =0.1 and (c) x = 0.2.

Temperature dependent magnetization measurements on single crystals of $Fe_{2-x}Co_xMo_3O_8$ (x = 0.25, 1)

The temperature dependent magnetization on single crystal of were carried out from 300 -5 K at external field of 0.1 T in H//c and H⊥c configuration. For x = 0.25, the antiferromagnetic ordering is observed at T_N = 58 K and for x = 1.0, spin orders at T_N = 48 K. The negative value of Curie-Weiss temperatures show the robustness of antiferromagnetic ordering.

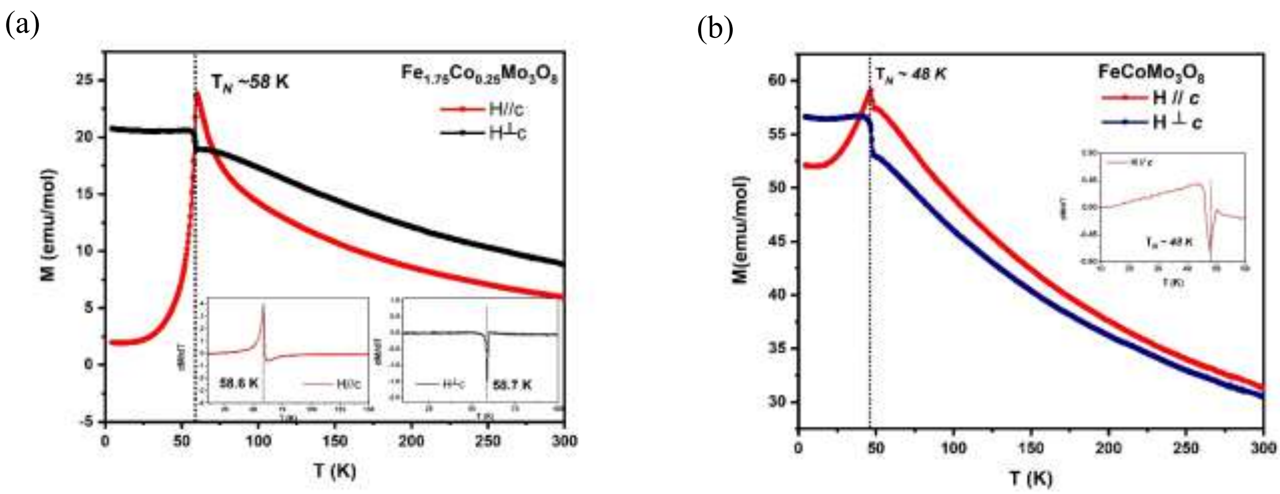

(c) (d)

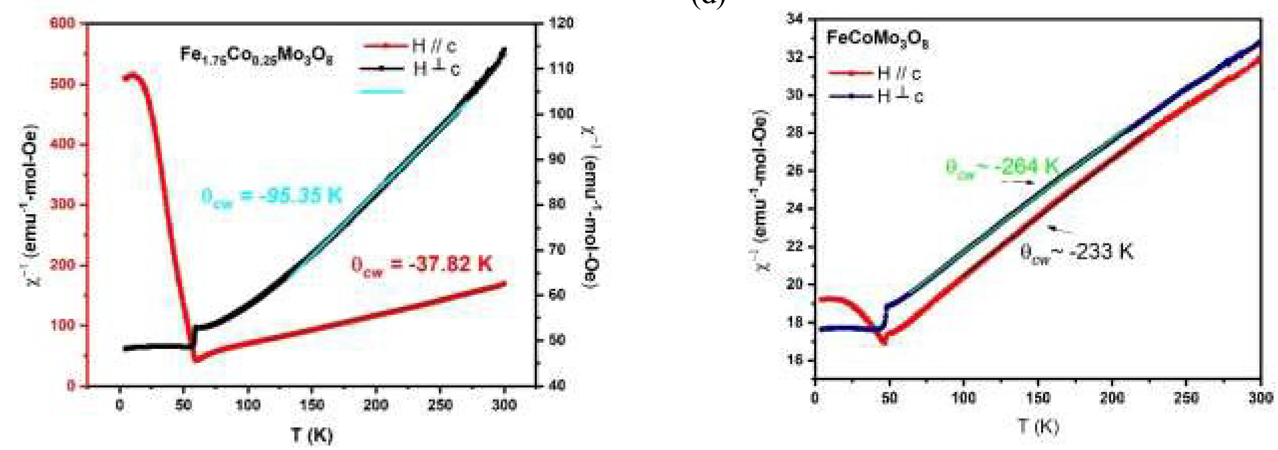

Figure 7. Temperature dependent magnetization measurements at 0.1 T on single crystal of $Fe_{2-x}Co_xMo_3O_8$ (a) x =0.25, (b) x = 1. (c) represents the inverse susceptibility curve as a function of temperature for (c) x = 0.25 and (d) x =1.

So these are the measurements which were carried out on single crystals and polycrystalline compound of $Mn_{2-x}Ni_xMo_3O_8$ and $Fe_{2-x}Co_xMo_3O_8$. at IMR. Tohoku university, Japan. For $Mn_2Mo_3O_8$ compound, the high-field magnetization, polarization and ESR data are analyzed and compiled in the form of manuscript along with the $Fe_2Mo_3O_8$ compound, where magnetization is analyzed and added to this in manuscript. Moreover, rest of the data are being analyzed for further establishments. So far, we have proposed manuscripts based on the measurements are following:

(1) On the Magneto-structural Signatures in $Mn_2Mo_3O_8$ Polar Magnets through high-field ESR and LT-SPXRD studies.

(2) Structural Evolution, High-Field magnetization, Electronic structure and Mössbauer Spectroscopic Studies in Polar Altermagnet $Fe_2Mo_3O_8$.

References:

[1] T. Kurumaji, S. Ishiwata, and Y. Tokura, Phys. Rev. X **5**, 031034 (2015).

[2] T. Kurumaji, S. Ishiwata, and Y. Tokura, Phys. Rev. B **95**, 045142 (2017).

[3] Q. Chen, A. Miyake, T. Kurumaji, K. Matsuura, F. Kagawa, S. Miyahara, Y. Tokura, and M. Tokunaga, Phys. Rev. B **109**, 094419 (2024).

Turpu Goverdhan Reddy, Tarun Pratap Singh, Guru Ghasidas Vishwavidyalaya, Bilaspur
E-mail : tg.reddy@ggu.ac.in, tarunpratap96@gmail.com

Unveiling Exotic Quantum Phenomena in Ternary Metal Pnictide-Based Intermetallics: Probing Topological States through Quantum Oscillations

This study investigates transport and magnetic properties of rare-earth pnictides (RETPn$_2$). Measurements show anisotropic, linear, nonsaturating giant magnetoresistance up to 2500% at 2 K. Hall data reveal multiband transport with electrons and high-mobility holes (~85,000 cm^{2}V^{-1}s^{-1}), indicating nontrivial fermiology driven by nonsymmorphic symmetry in this quantum material.

Layered pnictides containing Bi/Sb square nets have attracted significant attention as a class of materials hosting relativistic fermions. In compounds like AMnBi$_2$ and AMnSb$_2$ (A = Ca, Sr, Ba, Eu), the interplay of magnetism and spin–orbit coupling can break time-reversal symmetry and generate Weyl states. RAgBi$_2$ and RAgSb$_2$ compounds, featuring antiferromagnetic ordering at low temperatures. Their tunable magnetic and electronic properties make them ideal systems for exploring Dirac fermions coupled with rare-earth magnetism. The in-plane resistivity ρ(T) of REAgBi$_2$ exhibits metallic behavior over the entire temperature range (300–2 K). A clear anomaly is observed near the Néel temperature (T_n ≈ 11 K), where resistivity drops sharply due to the suppression of spin-disorder scattering associated with antiferromagnetic ordering. The low residual resistivity (~0.76 μΩ·cm) and high residual resistivity ratio (RRR ≈ 126) indicate excellent crystal quality. Magnetoresistance (MR) is large, anisotropic, and nonsaturating, reaching ~2500% for H ∥ c and ~1200% for H ∥ ab at 2 K. It shows an approximately linear dependence on magnetic field and decreases with increasing temperature. This behavior is consistent with Abrikosov quantum linear magnetoresistance, suggesting the presence of Dirac-like carriers. Hall resistivity measurements confirm multicarrier transport, with hole-dominated conduction at high fields and nonlinear behavior at low fields indicating contributions from both electrons and holes. Analysis reveals high hole mobility (~10^4–10^5 cm^{2}V^{-1}s^{-1}), supporting a semimetallic state with Dirac-like electronic behavior.

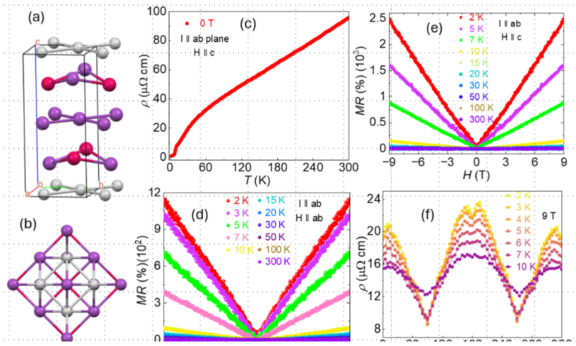

Fig. 1 (a) Layered tetragonal crystal structure of REAgPn$_3$ with square-net planes. (b) Top view of the square-net lattice. (c) Zero field In-plane resistivity ρ(T) from 2-300 K temperature. (d, e) Magnetoresistance for both H ∥ *ab* and H ∥ *c* field orientation. (f) Angular resistivity shows anisotropic magnetoresistance.

References

[1] J. Park, G. Lee, F. Wolff-Fabris, Y. Y. Koh, M. J. Eom, Y. K. Kim, M. A. Farhan, Y. J. Jo, C. Kim, J. H. Shim, and J.S. Kim, Phys. Rev. Lett. **107**, (2011)126402.

[2] S. Malick, H. Swiatek, M. J. Winiarski, and T. Klimczuk, Phys. Rev. B **111**, (2025) 045144.

Keywords: Crystal, metallic conductor, fermi surface
Haribrahma Singh, Department of Chemistry IIT Delhi.
E-mail: haribrahm@gmail.com

High Magnetic Field Heat Capacity on Fe-Based Molecular Magnets

Heat capacity measurements of the molecular magnets {Fe_{16}} and {Fe_{12}} were performed in magnetic fields up to 14.5 T. Isothermal heat capacity data, collected at 1.8 K as a function of the magnetic field, reveal broad anomalies consistent with the presence of weak crystal-field anisotropy and magnetic interactions.

Superexchange interactions in the molecular clusters {Fe16} and {Fe12} lead to the stabilization of ground states with spin values s = 20 and s = 8, respectively, as shown in previously measured magnetization data. In addition, {Fe16} exhibits clear evidence of a dipolar-coupling-driven phase transition below 1 K, as revealed by heat capacity measurements at low magnetic fields. This behavior is analogous to that observed in the related compound {Fe17} [1], [2].

During the experiments conducted at HFLSM in the period from January 4 to March 1, 2026, new isothermal heat capacity data were collected at 1.8 K for both Fe-based molecular magnets. Magnetic fields of up to 14.5 T, generated by the 15 T superconducting magnet (15TSM), were used in combination with the heat capacity setup developed by Dr. M. Akaki.

Fig. 1 shows the new data for {Fe16}, revealing a broad feature centered around B = 3 T, in agreement with measurements previously obtained using a PPMS system (Quantum Design) for magnetic fields up to 7 T. In the new data recorded for B > 7 T, no additional anomalies are observed.

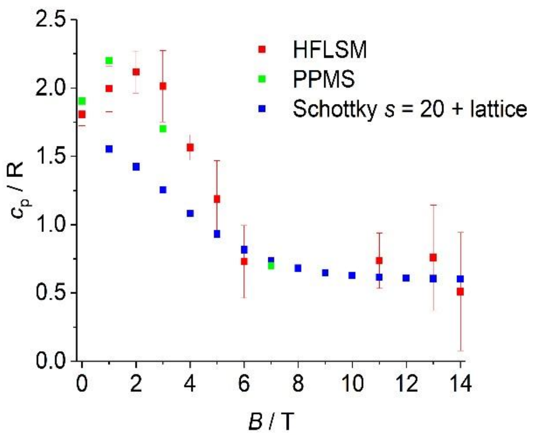

Fig. 1 Isothermal heat capacity data for {Fe_{16}}.

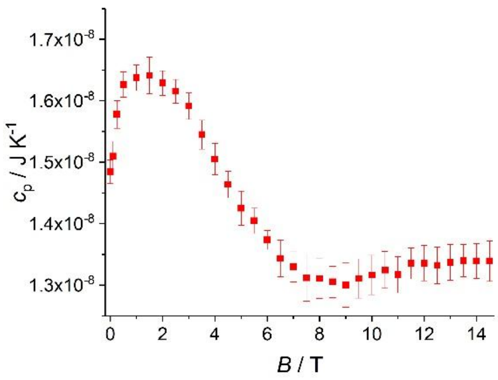

Fig. 2 Isothermal heat capacity data for {Fe_{12}}.

Similarly, Fig. 2 presents the new data for {Fe12}. A broad anomaly is observed around B = 2 T, while for fields above 8 T the heat capacity remains essentially constant, with no evidence of additional magnetic features within the studied field range. This behavior can be satisfactorily reproduced by parameterizing the interactions among the twelve Fe ions using six different exchange constants obtained from DFT analysis (not shown here). These results will be reported in a forthcoming publication that is currently in preparation.

References

[1] Evangelisti, M.; et al. Tunable dipolar magnetism in high-spin molecular clusters. Physical Review Letters, vol. 97, no. 16, pp. 167202, 2006.

[2] Gass, I.A.; et al. Cryogenic magnetocaloric effect in the Fe17 molecular nanomagnet. Polyhedron, vol. 52, pp. 1177–1180, 2013.

Keywords: calorimetry, specific heat, magnetism
David Gracia Alcalde, Universidad de Zaragoza, Zaragoza, Spain
E-mail: dgracia@unizar.es
https://orcid.org/my-orcid?orcid=0000-0002-3511-3510

Accepted No.	Chairperson or Committee Member	Title of Workshop	Place	Term
24WS3	Prof. Miyasaka	GIMRT Workshop: 1st International Conference on Molecular Spin Qubits toward Quantum Computer and Sensors (ICMSQ2025)	Sendai	2025.6.7-10
25WS1	Prof. Yamanaka	GIMRT Workshop: The 20th International Workshop on Biomaterials in Interface Science	Sendai	2025.8.1
25WS3	Assoc. Prof. Wada	GIMRT Workshop: 5th International Symposium on Nanoporous Materials by Alloy Corrosion (5th ISNMAC)	Sendai	2025.10.6-10.8
25WS4	Prof. Kato	ICC-IMR Workshop: IMR-JBNU-KIST Joint Symposium 2026	Sendai	2026.1.27-1.28
25KW1	Prof. Nojiri	ICC-IMR Workshop: KINKEN WAKATE 2025 Japan-India Material Science School for Young Scientists	Sendai	2025.11.17-11.19

IMR International Workshop: 1st International Conference on Molecular Spin Qubits toward Quantum Computer and Sensors (ICMSQ2025)

実行委員長：宮坂 等、名誉実行委員長：山下 正廣
学会事務局：高坂 亘、芳野 遼、西山 智貴

IMR International Workshop: 1st International Conference on Molecular Spin Qubits toward Quantum Computer and Sensors (ICMSQ2025)

Hitoshi Miyasaka, Masahiro Yamashita, Wataru Kosaka, Toru Yoshino, Tomoki Nishiyama
Institute for Materials Research, Tohoku University, Sendai 980-8577, Japan

Keywords: Molecular Spin Qubits, Quantum Computer, Quantum Sensors, Single-Molecule Magnets

Classical bits consist of 0 and 1, whereas quantum bits (qubits) are formed by the superposition of 0 and 1 ($\psi = a|0> + b|1>$). Qubits hold great promise for quantum computing and quantum sensors. To date, several types of qubits have been realized using superconducting loops, photons, quantum dots, trapped atoms, and nitrogen vacancies in diamond, among others. Each of these has its own advantages and disadvantages for practical applications. Recently, molecular spin qubits have emerged as a potential next-generation candidate due to (1) spin phase control via pulse ESR, (2) high spin-polarization of electron spin, and (3) high molecular designability. To make molecular spin qubits viable for real-world applications, we must extend the T1 and T2 times and achieve room temperature performance with long coherence by employing molecular designs, crystal lattice designs, and other strategies.

1. 緒言

古典的なビットは、0 と 1 の組み合わせから成っている。一方、量子ビットは 0 と 1 の重ね合わせから成っている（$\psi = a|0\rangle + b|1\rangle$）。量子ビットは、量子コンピューターや量子センサーなどへの展開が大いに期待されている。これまでに、超伝導ループ、光子（photon）、量子ドット、ダイヤモンド欠陥などが量子ビットの候補として研究されてきたが、いずれも一長一短がある。これに対して、ごく最近、分子スピンキュービットが注目を集めている。その特徴は、(1) パルス ESR によるスピン位相の制御、(2) 電子スピンの高いスピン偏極、(3) 分子設計の容易さ、などである。本国際会議では、分子スピンキュービット分野の世界トップの研究者 50 名を招待し、この分野の最前線の研究紹介と将来展望について議論した。

2. 会議の詳細

ICMSQ2025 は、2025 年 6 月 7 日～10 日に金研大講堂で開催された。プレナリー講演者 3 名および招待講演者 47 名は以下のとおりである。参加者総数は 15 ヶ国から 113 名であった。

(1) Masahiro Yamashita, Tohoku University, Japan, (2) Tadahiro Komeda, Tohoku University, Japan, (3) Stephen Hill, Florida State University, USA, (4) Toyo Kazu Yamada, Chiba University, Japan, (5) Nicolas Lorente, Donostia International Physics Center, Spain, (6) Christoph Wolf, Center for Quantum Nanoscience, South Korea, (7) Stefan Minasian, LBNL, USA, (8) Fernando Luis, University of Zaragoza, Spain, (9) Joe Zadrozny, Ohio State University, USA, (10) Alexey A. Popov, Germany, University of Dresden, Germany, (11) Shinya Hayami, Kumamoto University, Japan, (12) Talal Mallah, Universite Paris Saclay, France, (13) Bin Hu, University of Tennessee, USA, (14) Joris van Slageren, University of Stuttgart, Germany, (15) Deung-Jang Choi, Centro de Física de Materiales, Spain, (16) Marco Affronte, Università di Modena, Italy, (17) Shang Da Jiang, South China University of Technology, China, (18) Lorenzo Sorace, University of Firenze, Italy, (19) Mario Ruben, Karlsruhe Institute of Technology, Germany, (20) Eugenio Coronado, University of Valencia, Spain, (21) Masanori Wakizaka, Chitose Institute of Science and Technology, Japan, (22) Kazunobu Sato, Osaka Metropolitan University, Japan, (23) Yoji Horii, Nara Women`s University, Japan, (24) Nobuhiro

Yanai, Kyushu University, Japan, (25) Tetsuro Kusamoto, Osaka University, Japan, (26) Michael Wasielewski, Northwestern University, USA, (27) Michael Shatruk, Florida State University, USA, (28) Stefano Carretta, University of Parma, Italy, (29) Junjie Liu, University of Oxford, UK, (30) Susumu Takahashi, University of Southern California, USA, (31) Sandrine E M Heutz, Imperial College, UK, (32) Eufemio Moreno Pineda, Karlsruhe Institute of Technology, Germany, (33) Kasper S. Pedersen, Technical University of Denmark, Denmark, (34) Akimitsu Narita, OIST, Japan, (35) Selvan Demir, Michigan State University, USA, (36) Johannes Majer, University of Science and Technology of China, China, (37) Guillem Aromi, University of Barcelona, Spain, (38) Sabine Richert, University of Freiburg, Germany, (39) Dawid Pinkowicz, Jagiellonian University, Poland, (40) Ezekiel Johnston-Halperin, Ohio State University, USA, (41) Ramaswamy Murugavel, IIT-Bombay, India, (42) Sanjit Konar, IISER Bhopal, India, (43) Eva Rentschler, University of Mainz, Germany, (44) Annie Powell, Karlsruhe Institute of Technology, Germany, (45) Matthew Cliffe, University of Nottingham, UK, (46) George Christou, University of Florida, USA, (47) Valentin Dediu, CNR-ISMN, Italy, (48) Vignesh Kuduva R, IISER Mohali, India, (49) Danna Freedman, MIT, USA, (50) Andreas Heinrich, Ewha Woman`s University, South Korea

初日の宮坂等教授による開会あいさつに続き、シカゴ大学の Professor David D. Awschalom により、“Creating and Controlling Spin Qubits Through Molecular Engineering”と題したプレナリー講演が行われた。金属錯体や無機物を用いた量子ビットについて、基礎から応用まで多くの実験データに基づいた最先端の講演がなされ、本講演により世界における分子スピンキュービット研究の最前線の状況を把握することができた。続いて、3 名の招待講演者から、走査型トンネル顕微鏡（STM）および走査型トンネルスペクトロスコピー（STS）を用いた単分子磁石や分子磁石に関する ESR-STM の報告が行われた。低温における実験成功が報告され、実用化への道筋が示されるとともに、多様な観点から活発な議論が行われた。コーヒーブレイク後には、3 名の講演者からパルス ESR を用いた分子スピンキュービットの観測に関する報告があり、どのような化合物が量子ビットに適しているかについて、化学的観点から議論が行われた。ランチ後の午後には、単分子量子磁石に関する講演が行われ、磁気ヒステリシス温度の向上に関する研究が紹介された。有機ラジカルを配位子や架橋基に用いた試みが発表され、それを受けて理論的解析に関する報告も行われ、実験研究者と理論研究者の間で活発な議論が交わされた。コーヒーブレイク後には、有機ラジカルを用いた 2 次元および 3 次元の MOF・COF におけるスピンキュービットに関する報告があり、量子コンピューターや量子センサーへの応用可能性について議論が行われた。

2 日目には、MIT の Professor Danna Freedman によるプレナリー講演“Molecular Color Centers”が行われた。金属錯体の光励起を利用した量子センサーに関する報告であり、化合物の種類や測定手法について多くの質問が寄せられた。同氏の優れた講演に対し、日本化学会 BCSJ Lectureship Award が授与された。コーヒーブレイク後には、量子ビット候補として、高スピン型 Ni(II)錯体、$S = 1/2$ を有する第一遷移金属錯体、有機金属錯体、金属内包フラーレンなど、多様な化合物が紹介され、それぞれのスピンキュービット特性について報告がなされた。これに対し、化合物の安定性や取り扱いの容易さなどに関する質疑が行われた。ランチ後には、単分子量子磁石を超伝導基板上に蒸着させた量子センサー応用に関する報告があり、議論では動作温度の課題が指摘された。コーヒーブレイク後には、励起スピンの緩和過程に関する報告が行われ、その将来展望について議論がなされた。その後、3 次元 MOF へのスピンドーピングによる量子ビット生成や、金属錯体を用いた量子ビットの構築と性能評価に関する報告が行われ、分子設計に関する議論が活発に行われた。

3 日目には、基板上に蒸着された量子ビットの挙動、有機ラジカルを用いた量子ビット挙動、ナノリボンやナノグラフェンを用いた量子ビット実現の可能性に関する講演が続いた。分子量子ビットの特徴である高い設計自由度に関する報告に対し、より優れた分子設計の指針について議論が行われた。コーヒーブレイク後には、希土類金属錯体を用いた量子ビットに関する合成、基板上での ESR-STM 測定、理論計算に関する報告が行われ、それぞれの立場から最適な化合物設計について議論が行われた。最後に、熊本大学の速水真也教授により、

“Molecular Spin Qubit Behavior in Spin Crossover Systems”と題した講演が行われ、その優れた内容に対して「リガク国際賞」が授与され、授賞式が執り行われた。

最終日には、単分子量子磁石を用いた量子スピンビットの合成および測定に関する報告が行われ、活発な議論がなされた。最後に、ドイツ・カールスルーエ工科大学の Professor Mario Ruben によるプレナリー講演“Nuclear Spin Qubits for Implementing Quantum Gates and Algorithms”が行われ、単分子量子磁石の核スピンを用いた量子スピンキュービットに関する基礎から応用まで幅広い講演に、参加者から感嘆の声が上がった。

3. 今後の展望

以上のように、第 1 回 ICMSQ2025 は東北大学金属材料研究所において成功裏に終了した。これを受け、2 年後の ICMSQ2027 を、2027 年 11 月 30 日から 12 月 2 日に仙台国際センターで開催することが決定した。さらに、関連分野である第 1 回先端単分子量子磁石国際会議（ICSMM2027）も、ICMSQ2027 に連続して 12 月 3 日から 12 月 5 日まで同会場にて開催される予定である。

両分野ともに、今後も日本の研究が世界をリードしていくことが大いに期待される。

4. 終わりに

金研からのご支援により、ICMSQ2025 は大成功に終わることができた。多くの参加者から第 2 回目の 2027 年開催予定の ICMSQ2027 に参加したいとのメールをいただいた。

The 20th International Workshop on Biomaterials in Interface Science

研究代表者：東北大金研 山中謙太
研究分担者：東北大金研 加藤秀実　東北大歯学 陳鵬 金高弘恭 小坂健
東北大工 成島尚之 東京科学大 川下将一

Kenta YAMANAKA[1,2], Hidemi KATO[1,2], Peng CHEN[3], Hiroyasu KANETAKA[2,3], Ken OSAKA[2], Takayuki NARUSHIMA[2,4], Masakazu KAWASHITA[5]

[1]Institute for Materials Research, Tohoku University, 2-1-1 Katahira, Aoba-ku, Sendai 980-8577, Japan

[2]Graduate School of Biomedical Engineering, Tohoku University, 6-6-12, Aramaki Aza Aoba Aoba-ku, Sendai, Miyagi 980-8579, Japan

[3]Graduate School of Dentistry, Tohoku University, 4-1 Seiryo-machi, Aoba-ku, Sendai 980-8575, Japan

[4]Graduate School of Engineering, Tohoku University, Aoba-yama 02, Aoba-ku, Sendai 980-8579, Japan

[5]Laboratory for Biomaterials and Bioengineering, Institute of Science Tokyo, 2-3-10 Kanda-Surugadai, Chiyoda-ku, Tokyo 101-0062, Japan

1. 概要

高齢化社会の進展に伴い、人工骨や人工歯をはじめとする人体部位を人工製品で代替するニーズが高まり、生体材料と人体をつなぐ Intelligent Interface に関する研究は一層重要性を増しています。生体材料には、生体適合性を維持しつつナノからマイクロスケールにおける機械的・生物学的機能を精密に制御することが求められ、特に材料科学の知見がその基盤を支えています。こうした課題に対応するため、東北大学では 2011 年より金属材料研究所、大学院歯学研究科、大学院医工学研究科が連携し、"Innovative Research on Biosis-Abiosis Intelligent Interfaces"を推進しています。本プロジェクトでは、新規合金やセラミックス、
高分子など多様な材料を対象に、機能性・耐久性・生体親和性を兼ね備えた次世代生体材料の開発を進めるとともに、それを応用した医療機器や診断技術にも注力しています。2025年 8 月 1 日に開催された"The 20th International Workshop on Biomaterials in Interface Science"では、生体材料、歯学、生体医工学分野の第一線で活躍する 4 名の研究者を招き、さらに東北大学や東京科学大学の研究者・学生による 22 件の口頭発表が行われました。

2. 内容

対面開催を中心とし東北大学金属材料研究所講堂を会場併用したハイブリット形式で開催しました。4 つのセッション分け、それぞれ招待講演、若手研究者ならびに学生による口頭発表を行いました。招待講演者と発表題目は以下の通りです。

Biomaterials:

招待講演者　Chun-Li Lin (National Yang Ming Chiao Tung University)

研究題目　“Macro Optimized and Micro Bionic Metal 3D Printed Implants: Meeting Unmet Clinical Needs and FDA Standards”
Biomedical Engineering:
招待講演者　Wei-Ning Lee(The University of Hong Kong)
研究題目　“Ultrasound Elastographic Methods for In Vivo Assessment of Cardiovascular Tissue Anisotropy”
Young Investigator:
招待講演者　Zhang Chengfei(The University of Hong Kong)
研究題目　“Interactions of ECs and DPSCs on DPSC-induced Vascular Maturation”
Oral Health Care:
招待講演者　Han-Cheol Choe(Chosun University)
研究題目　“Functional Surface Modification for Dental Implant”

参加者は 66 名（オンサイト 54 名、オンライン 12 名）であり、発表では金属材料やバイオセラミックスの微細構造制御、表面改質技術、細胞応答との相互作用といった材料科学的視点からの最新成果が共有されました。分野を超えた議論を通じて新しい研究連携を促進するとともに、若手研究者や学生にとって貴重な学習・交流の機会となりました。

3. 謝辞

TOP

本ワークショップは、東北大学金属材料研究所国際・産学連携インヴァースイノベーション材料創出プロジェクトが主催し、GIMRT の助成により実施されました。運営にご支援いただいたすべての方に謝意を表します。今後も材料科学を中核に据えた学際的研究を深化させ生体材料と医療技術の革新に寄与して参りたいと思います。

5th International Symposium on Nanoporous Materials by Alloy Corrosion

研究代表者：東北大金研　和田　武

Takeshi WADA
Institute for Materials Research, Tohoku University, Sendai 980-8577, Japan

Keywords: dealloying, nanoporous material, porosity, bicontinuous structure, surface area

Nanoporous metals produced via dealloying represent an emerging class of materials, characterized by a bicontinuous network of solid ligaments ranging from nanometers to micrometers. By integrating nanoscale properties into macroscopic components, these materials offer unique opportunities for engineering applications. Despite their long history, fundamental challenges remain in understanding dealloying mechanisms, topological evolution during coarsening, and the critical links between processing parameters and resulting properties. The 5th International Symposium on Nanoporous Materials by Alloy Corrosion (ISNMAC), held in Sendai, Japan, provided a premier platform for world-leading researchers to exchange innovative ideas. The symposium focused on diverse dealloying processes—including electrochemical, vapor-phase, liquid-metal, and solid-state methods—alongside novel fabrication techniques. Key topics encompassed the morphological evolution of nanoporous microstructures, their mechanical behavior, and functional applications in areas such as catalysis, sensing, and energy storage and conversion.

1. 緒言

合金の脱成分 (dealloying) によって生成するナノポーラス金属は、ナノからマイクロメートルオーダーのリガメントがネットワークを形成する共連続構造を特徴とする。この構造体は、1 cm^3 あたり 10^{15} 個を超える極めて膨大な数のリガメントを有し、ナノスケール特有の性質をマクロな材料として活用できるため、触媒やセンサーなど多様な工業応用が期待されている。脱成分は材料工学において長い歴史を持つが、その組織形成メカニズムには未解明な点が多い。特に、脱成分過程における熱力学、トポロジー、リガメント粗大化機構の解明、さらには作製条件・微細構造・材料特性の相関関係を明らかにすることが実用化の促進には不可欠である。International Symposium on Nanoporous Materials by Alloy Corrosion（ISNMAC）は、この分野の研究者が一堂に会し、科学的知見の交換と相互交流を図ることを目的とした国際シンポジウムである。２０１４年のドイツでの発足を皮切りに、第２回ドイツ（２０１６年）、第３回アメリカ（２０１９年）、第４回ドイツ（２０２３年）と欧米で継続的に開催されてきた。本会議は、世界各国の著名な研究者が集う当該分野で最も認知度の高い国際会議の一つ（６０～７０名規模）である。第５回目となる今回は、実行委員長として本所の加藤秀実教授、オーガナイザーとして研究代表者（和田）、Prof. Ilya Okulov（ドイツ）、Prof. Yu-chen Karen Chen-Wiegart（アメリカ）の運営体制で、２０２５年１０月６日～８日に仙台（仙台国際ホテル）にて開催した 。

図１．第５回 ISNMAC のポスター

2. 開催内容

２０２４年５月に実行委員会を行い、第５回 ISNMAC の開催場所を仙台国際ホテルとすること、およびトピックを（１）各種脱成分プロセス、（２）ナノポーラス構造の形態発達、（３）機械的性質、（４）階層構造、（５）先端分析技術、（６）シミュレーション、（７）機能性、（８）応用とすることに決定した。これに基づいて２０２４年１０月にシンポジウムウェブサイトを作成、公開して参加者を募った。その結果、口頭発表、ポスター発表の合計約６０件の投稿がありプログラム編成（図２）を行った。

● １日目

１日目は、実行委員長の加藤秀実教授による開会挨拶に続き、ハンブルグ工科大学（ドイツ）の Prof. Patrick Huber による BlueMat - Water-Driven Materials と題された基調講演が行われた。講演では“If you can do it with water, do it with water.”をモットーに、ナノポーラス金属と水を巧みに組み合わせた機能材料開発の最前線が紹介された。その後は、ナノポーラス金属の照射耐性や触媒・アクチュエータ応用に関する５件の招待講演と４件の一般講演が行われた。夕刻のポスターセッションでは、１７名の若手研究者が登壇してポスタースラム（２分間のショートプレゼン）に臨み、引き続き各自のポスター発表に移行し活発な議論が交わされた。

● ２日目

２日目は南方科技大学（中国）の Prof. Mingwei Chen による Thermodynamics and Kinetics of Vapor Phase Dealloying と題する基調講演が行われた。講演では、合金から高蒸気圧元素を揮発させることで低蒸気圧元素のナノポーラス金属を作製する技術、およびその生成機構および制御因子を熱力学と速度論の両面から解明した最新の研究成果が発表された。その後は、ナノポーラス金属の力学特性や相変態、形態シミュレーション、ハイエントロピー合金、溶融塩脱成分などの多岐にわたるテーマについて、５件の招待講演と６件の一般講演が行われた。

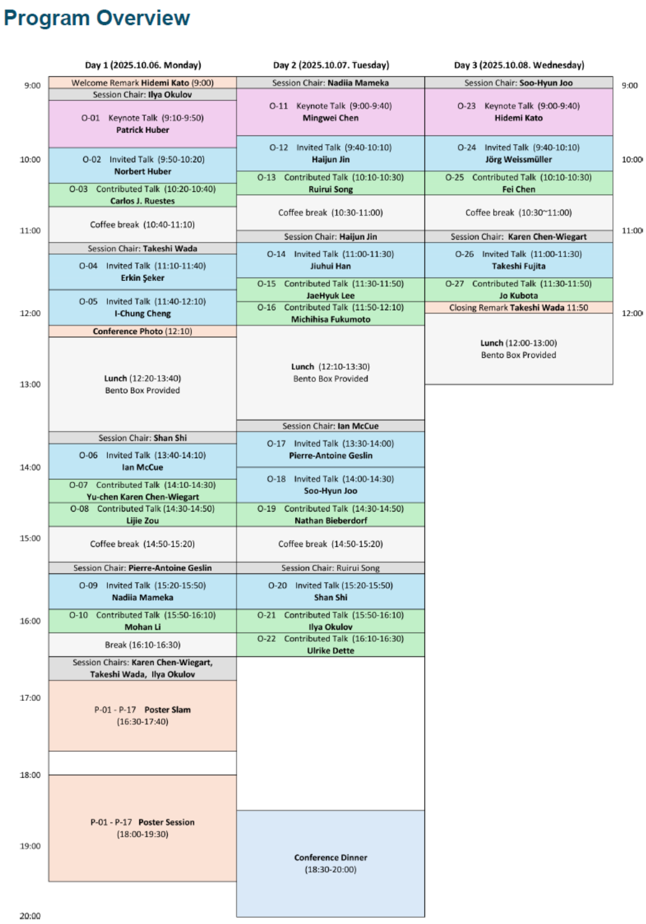

図２．第５回 ISNMAC プログラム

● ３日目

３日目は本所の加藤秀実教授による Immiscible Dissimilar Material Joints using Liquid Metal Dealloying と題する基調講演が行われた。講演では、鉄のマグネシウムのように合金化や化合物形成が無く、接合困難な異材に対して脱成分を適用することで、異材界面に両者が複雑に絡み合ったミクロ複合組織を形成させて接合を達成する先駆的な取り組みが披露された。その後は、ナノポーラス金属の水素貯蔵特性や超多成分ナノポーラス合金触媒、水素発生触媒への応用をテーマとした２件の招待講演と２件の一般講演が行われた。最後に研究代表者（和田）の閉会挨拶を以て全プログラムが終了した。閉会後には、希望者を対象とした片平キャンパスツアーおよび金属材料研究所内のラボツアーが開催され、盛況のうちに全日程を終えた。

3. まとめ

２０２５年１０月６日～８日の３日間にわたり、仙台国際ホテルにて第５回 ISNMAC を開催した。今回のシンポジウムでは、世界８カ国から当該分野を牽引する研究者５１名（内、若手研究者３２名、女性研究者１６名）が一堂に会し、４５件の意欲的な研究発表が行われた。議論の対象は、脱成分の基礎となる熱力学や動力学の解明から、触媒、エネルギー貯蔵、機械的特性、先端分析技術、高度なシミュレーションや機械学習に至るまで多岐にわたった。また、若手研究者によるポスターセッションや研究所ツアーも実施され、学術的知見の深化と国際的な研究ネットワークの強化が図られた。過去４回の ISNMAC は欧米で開催されてきたが、今回を仙台で開催できたことは、東北大学および金属材料研究所が脱成分およびナノポーラス金属の研究における世界的な中核拠点であることを国際コミュニティに印象付ける絶好の機会となった。今回のシンポジウムを通じて醸成された人的ネットワークを礎とし、GIMRT の枠組みを積極的に活用することで、国境を越えた国際共同研究が加速することが期待される。

謝辞

本シンポジウムの実施にあたり、東北大学金属材料研究所・加藤研究室・伊藤佐江子秘書には多大なご尽力をいただいた。この場を借りて深くお礼を申し上げます。

参考資料

参加者全員の集合写真

TOP

10/6 講演の様子 (Prof. Y.-c. K. Chen-Wiegart)

10/6 ポスターセッションの様子

10/7 基調講演の様子 (Prof. M.W. Chen)

10/8 招待講演の様子 (Prof. J. Weissmüller)

IMR-JBNU-KIST Joint Symposium 2026

This report summarizes the IMR–JBNU–KIST Joint Symposium, which aimed to promote research exchange and collaborative activities among the participating institutions. The symposium provided a platform for researchers from Japan and Korea to present recent advances in materials science, discuss emerging research topics, and explore opportunities for joint projects and long-term international collaboration.

The IMR–JBNU–KIST Joint Symposium was held to strengthen academic cooperation and promote sustainable research exchange among the Institute for Materials Research (IMR), Tohoku University, Jeonbuk National University (JBNU), and the Korea Institute of Science and Technology (KIST). The symposium was organized based on the institutional partnerships established through the Memorandum of Understanding between Tohoku University and JBNU and the long-standing academic exchange agreement between IMR and KIST. Building upon these collaborative frameworks, the symposium aimed to provide a platform for sharing recent research achievements, identifying common research interests, and fostering long-term international collaboration in materials science and engineering.

Fig.1. Group photo of participants at the IMR–JBNU–KIST Joint Symposium 2026.

The symposium began with opening remarks delivered by Prof. Takahiko Sasaki, Director of the Institute for Materials Research at Tohoku University, and Prof. Man Young Kim, Dean of Engineering at Jeonbuk National University. In their greetings, both speakers emphasized the importance of international academic collaboration and expressed their expectations that the symposium would serve as a catalyst for strengthening research partnerships among the participating institutions.

Fig. 2. Prof. Chang Kyu Jeong from JBNU delivering his presentation.

Following the opening session, a series of invited lectures were presented by leading researchers from JBNU, IMR, and KIST. The presentations covered a broad spectrum of interdisciplinary topics in advanced materials science. Researchers from JBNU introduced their recent work on hierarchical nanostructured materials, layered nanocomposites for solar-driven desalination, meta-composites, mesoporous inorganic materials, dielectric capacitors, and two-dimensional metal nanosheets for conductive film applications. In addition, research on large language models applied to materials science and advanced coating and surface engineering technologies for next-generation steel was presented.

KIST researchers contributed presentations on applied materials engineering and advanced composite technologies. Their talks addressed structural integrity evaluation of composite materials using nondestructive testing, design and manufacturing strategies for ultra-light hybrid composites for extreme environments, and functional composites for neutron shielding through the functionalization of boron nitride nanotubes.

Researchers from IMR presented their latest studies on functional materials and magnetic materials, including layered manganese dioxide for heat-storage applications utilizing environmental water vapor, spin–orbit torque operations in synthetic antiferromagnets, and chirality control and detection in metallic helimagnets. These presentations highlighted IMR's strengths in advanced materials design and fundamental physical mechanisms in functional materials.

Throughout the symposium, active discussions took place among participants regarding emerging research trends and potential areas of collaboration. The workshop provided valuable opportunities for participants to exchange technical expertise, identify common research interests, and explore possibilities for future joint research projects and researcher exchange programs.

Overall, the IMR–JBNU–KIST Joint Symposium successfully brought together researchers from the three institutions and established a strong foundation for future international collaboration. The discussions and interactions during the symposium are expected to contribute to the development of joint research initiatives and to strengthen the global research network in advanced materials science.

Fig. 3. Presentation by Dr. Seokhoon Ahn from KIST.

Fig. 4. Prof. Takeshi Seki from IMR delivering a presentation.

Fig. 5. Group photo of JBNU and KIST participants with Prof. Takahiko Sasaki, Director of IMR.

Keywords: metal, polymer, spintronic
Seungkyun Yim (Cooperative Research and Development Center for Advanced Materials)
E-mail: yim.seungkyun.a3@tohoku.ac.jp
https://www.crdam.imr.tohoku.ac.jp/english/

Japan-India Materials Science School for Young Scientists 2025 Successfully Concludes

The Institute for Materials Research (IMR) at Tohoku University hold an annual Materials Science School for Young Scientists. This year marked the 20th time the event has been held since its inception in March 2005. In 2025, as a special initiative focusing on the rapidly expanding collaborative research between Japan and India, the "Japan-India Young Scientists Materials Science School 2025" was held at the IMR Auditorium from November 17 to 19, welcoming approximately 40 participants, including 22 attendees from India (both on-site and online).

Expert Lectures and International Exchange

The three-day school featured lectures delivered by specialists in the field. A total of six lecturers contributed their expertise: three lecturers from India lectured online, while from Japan, two lecturers lectured on-site and one lecturer presented online.

Lecturers:

Prof. Ashok Kumar Ganguli,
Indian Institute of Technology- Delhi (Online)

Dr. Kaustuv Manna,
Indian Institute of Technology- Delhi (Online)

Prof. Mukannan Arivanandhan,
Anna University (Online)

Assoc. Prof. Seigo Soma,
AIMR, Tohoku University (On-site)

Prof. Masashi Watanabe,
IMR, Tohoku University (Online)

Assoc. Prof. Kei Kamada,
IMR, Tohoku University (On-site)

Participants listened attentively to the diverse presentations over the course of the three days, fostering a broad intellectual exchange.

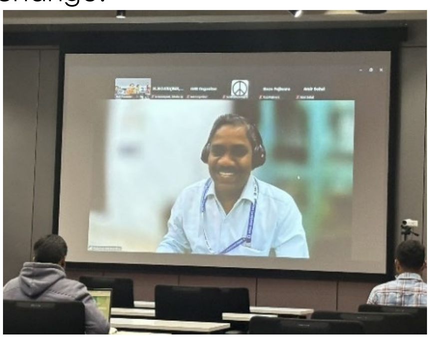

Valuable On-Site Experience for Indian PhD Students

A notable highlight was the attendance of five selected PhD students from India, who traveled to Japan specifically for the school. Beyond attending the lectures, they gained valuable, multi-faceted experiences. This included touring various experimental facilities within IMR and visiting Tohoku University's cutting-edge Nano Terrace facility. This successful in-person engagement further deepened the international exchange among the young scientists, providing them with essential practical exposure.

Japan-India Material Science School for Young Scientists 2025
Date: November 17-19, 2025
Venue: Institute for Materials Research, Tohoku University and Online Hybrid

Program

November 17		
10:00-10:30	Onsite attendant Gathering Welcome and guidance	
10:30-11:30	Exchange 1	Short Presentation by Onsite Attendants
11:30-13:00	Break	
13:00-14:00	Lecture 1	**Prof. Mukannan Arivanandhan, Anna University** *Thermoelectric Materials: From Fundamentals to Future Applications"*
14:00-14:30	Break	
14:30-15:30	Lecture 2	**Assoc. Prof. Manna Kaustuv, IIT- Delhi** *Topology in Magnetism and Transport*
15:30-16:00	Break	
16:00-16:30	Exchange 2	**Dr. Kushwaha Varun Kumar, IMR** *My Research life in Japan and IMR*
16:30-17:00	Free Discussion	

November 18		
9:30-10:30	Laboratory Visit	High Magnetic Field Laboratory for Superconducting Materials
10:30-11:00	Break	
11:00-12:00	Lecture 3	**Prof. Masashi Watanabe, Tohoku University** *Tunneling Electron Microscope for Materials Science*
12:00-13:30	Break	
13:30-14:30	Lecture 4	**Prof. Ashok Kumar Ganguli, IIT- Delhi** *Material Synthesis for Strongly Correlated Electron and 2D Materials,*
14:30-15:00	Break	
15:00-16:00	Lecture 5	**Assoc. Prof. Kei Kamada, Tohoku University** *Physics and Chemistry of Scintillators*
16:00-17:30	Free Discussion	
17:30-19:00	Mixer	

November 19		
9:30-10:15	Laboratory Visit	Cooperative Research and Development Center for Advanced Materials
10:30-11:30	Lecture 6	**Assoc. Prof. Seigo Soma, Tohoku University** *Synchrotron radiation for Materials Science*
11:30-11:45	Closing	
11:45-12:50	Break	
12:50-15:00	Laboratory Visit	Nano Terasu Laboratory Toor

Accepted No.	Title・PI・Affiliation	Proposed Research	PI at IMR	Term
2024PJT1	Prof. Oleksandr Tovstolytkin・Institute of Magnetism of the NAS of Ukraine and MES of Ukraine	Development of Pulsed Magnetic Field System for Functional Magnetic Materials	Prof. Nojiri	FY2024-2025

Development of Pulsed Magnetic Field System for Functional Magnetic Materials

A Pulsed High Magnetic Field Measurement System has been developed, and its parameters have been tested. The System's ability to produce pulsed magnetic fields of 10–16 T has been confirmed, as has the temperature range achievable using the system (77–350 K). It has been demonstrated that the System's measurement capabilities allow for the measurement of magnetic moment, magnetoresistance, dielectric permittivity and magnetocaloric effect parameters. Further tests performed on representative samples of magnetic shape memory alloys confirmed the planned measurement capabilities. The System had been transferred to the V. G. Baryakhtar Institute of Magnetism of the National Academy of Sciences of Ukraine in Kyiv.

1. Introduction

Magnetic shape memory alloys (MSMAs) represent a unique class of functional materials that combine strong magneto-mechanical coupling with rapid, reversible deformation under external stimuli. Their ability to undergo large strains driven by magnetic fields makes them highly promising for applications in actuators, sensors, and energy conversion systems. However, the fundamental mechanisms governing their behavior – such as twin boundary motion, magnetic domain reorientation, and phase transformations – are strongly field-dependent and often nonlinear, particularly at elevated magnetic field strengths. As a result, understanding their full functional potential requires experimental investigation beyond low-field regimes.

High magnetic field measurements are therefore essential for accurately characterizing the intrinsic properties of MSMAs and revealing phenomena that remain inaccessible at moderate fields. Such measurements enable the determination of saturation magnetization, critical switching fields, magneto crystalline anisotropy, and field-induced phase transitions with greater precision. Moreover, they provide insight into energy barriers and hysteretic effects that directly impact material performance and efficiency in real-world applications. By extending the experimental parameter space, high-field studies play a crucial role in both validating theoretical models and guiding the design of advanced magnetic shape memory materials with optimized functional properties.

The aim of this work was to put into operation the Pulsed High Magnetic Field Measurement System developed by Prof. Hiroyuki Nojiri and his group at the Institute for Materials Research (Tohoku University) and carry out test measurements on the samples of magnetic shape memory alloys. The next step consists in the installation of the System in the V.G. Baryakhtar Institute of Magnetism of the NAS of Ukraine in Kyiv (Ukraine).

2. Experimental results

The first phase of the experiments involved examining the working parameters of the Pulsed High Magnetic Field Measurement System (Fig. 1a). The System's ability to produce pulsed magnetic fields of 10 – 16 T was confirmed. The temperature range achievable using the System was also tested. It was concluded that the reliable operating temperature range was 77–350 K.

During the first phase of testing the System's parameters, it was demonstrated that the System's measurement capabilities allow for the measurement of magnetic moment, magnetoresistance, dielectric permittivity, and magnetocaloric effect parameters. During the project implementation, all System parameters were calibrated.

Given that the System allows for the measurement of all these parameters in strong magnetic fields and over a wide temperature range, this makes it unique for experimental studies, especially for understanding the behavior and processes in complex magnetic systems including magnetic shape memory alloys.

Further tests were performed on representative samples of magnetic shape memory alloys ($Ni_{50}Mn_{38}Sb_{12}$, $Ni_{50}Mn_{37.5}Sn_{12.5}$ and $Ni_{41}Co_9Mn_{39}Sb_{11}$) in order to evaluate the measurement capabilities. The magnetic, magnetoresistance and magnetocaloric parameters were measured. It was demonstrated that the measured parameters correlate with those reported in the literature [1,2]. Figure 1(b), for example, shows the magnetization versus magnetic field dependence for a $Ni_{41}Co_9Mn_{39}Sb_{11}$ sample.

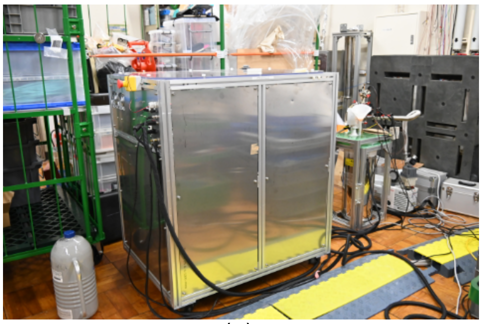

(a)

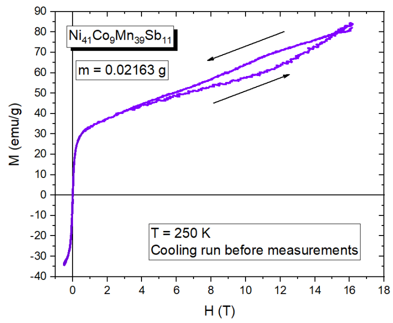

(b)

Fig. 1. (a) Pulsed High Magnetic Field Measurement System – a general view. (b) Magnetization vs magnetic field dependence for a $Ni_{41}Co_9Mn_{39}Sb_{11}$ sample, obtained with the use of the System.

The next phase involved transferring the System to the V. G. Baryakhtar Institute of Magnetism of the National Academy of Sciences of Ukraine in Kyiv. The system was successfully transported to Kyiv. It was unloaded at the Institute of Magnetism an installed and assembled for operation. (Fig. 2).

3. Conclusions

The Pulsed High Magnetic Field Measurement System developed at the Institute for Materials Research (Tohoku University) has been put into operation and its parameters have been examined. It has been confirmed that the measurement capabilities correspond to those planned. Test measurements on the samples of magnetic shape memory alloys confirmed the system's excellent performance. The system was transferred to Kyiv and it is in commissioning at the V. G. Baryakhtar Institute of Magnetism of the National Academy of Sciences of Ukraine in Kyiv.

Fig. 2. Transportation and further works on the installation of the Pulsed High Magnetic Field Measurement System at the V. G. Baryakhtar Institute of Magnetism of the National Academy of Sciences of Ukraine in Kyiv (https://imag.kyiv.ua/index.php/en/japan-grad.html).

4. Contributions by young researchers

Dr. Dmytro Velyhotskyi (35 years old), a junior researcher at the V. G. Baryakhtar Institute of Magnetism of the National Academy of Sciences of Ukraine, took part in testing the system in Japan. He will operate the System and perform measurements in Ukraine.

References

1. Rie Umetsu, Xiao Xu, Wataru Ito *et al.*: Metals **4** (2014) 609.
2. Anna Kosogor, Rie Umetsu, Vladimir Golub *et al.*: J. All. Comp. **988** (2024) 174130.

Keywords: magnetism, high magnetic field, calorimetry
Hiroyuki Nojiri (Magnetism Division)
E-mail: Hiroyuki.nojiri.e8@tohoku.ac.jp
https://www.hfpm.imr.tohoku.ac.jp

ICC-IMR FY2025
Activity Report

Edited by ICC-IMR Office
Published in September, 2026

Contact:

International Collaboration Center,
Institute for Materials Research (ICC-IMR),
Tohoku University
2-1-1 Katahira Aoba-ku, Sendai, 980-8577, Japan
TEL&FAX: 81-22-215-2019
Email: icc-imr@grp.tohoku.ac.jp

TOP